Chapter 4
Heat Release Rates in Tunnels

Abstract An overview of heat release rates (HRRs) for different vehicles driving through tunnels is presented. The focus is on understanding fire development and the influences of tunnel conditions on the HRR. The HRR describes the fire development in the form of energy release given in megawatts (MW) over a given time period. The chapter presents the basic theory of burning of fuels and summarizes the HRR for different types of vehicles, solid materials, and liquids. Influences of different physical parameters such as tunnel construction or ventilation on the HRR are addressed. The HRR is also given as a value per square metre of exposed fuel surface area.

Keywords Heat release rate (HRR) · Vehicles · Ventilation · Fuel · Burning rate · Surface area

4.1 Introduction

The tunnel length and the traffic density are usually the key design parameters when setting the level of safety in road tunnels. In more advanced engineering design of the fire protection systems, the HRR of the vehicles using the tunnel becomes an important input. In rail tunnels, engineering analysis is based on risk analysis and creation of a design fire for a given train. The HRR depends on factors such as the ignition source and vehicle type, their geometry and size, material type, the geometry of the tunnel, and the ventilation conditions. Furthermore, separations between vehicles are very important in relation to fire spread. The geometric configuration and proximity of fuels within a fuel package are also expected to significantly affect fire spread. For fire testing, fuel packages can be both real vehicles and mock-ups with arranged fuels such as pool fires or piled wood pallets.

Experience from large tunnel fires shows that the HRR is the most important parameter for describing the development and consequences of a fire. The HRR physically correlates to the mass burning rate of fuel and to the production of heat, smoke, and gases. In the engineering design of ventilation and evacuation systems, as well as the structural strength of a tunnel, the HRR is a key parameter. The design parameters usually involve tabulated peak HRR values in MW [1, 2]. In Chap. 6, design fires and curves are discussed in more detail.

H. Ingason et al., *Tunnel Fire Dynamics,* DOI 10.1007/978-1-4939-2199-7_4

In order to obtain an overview of the relevance of these tabulated design data, a summary of all available HRRs for vehicles and other type of fuels used in tunnels is needed. Results from experimental tests may vary considerably, even if the setup is similar. This is because not all factors can be exactly controlled. Using HRR results from different fire tests therefore, requires caution and wariness.

Compilations of HRR results for tunnel fires have been presented by the authors and others. This includes the overview given by Ingason [3] of HRRs of different vehicles until 2001 and the work in 2005 where Lönnermark and Ingason [4, 5] presented a compressed summary of peak HRRs and corresponding ceiling temperatures from large-scale tunnel fire tests. In 2006, Ingason [6] compiled and described most of the large-scale test data found in the literature, including HRR and gas temperatures; and, in the 2008 edition of the society of fire protection engineers (SFPE) Handbook of Fire Protection Engineering, Babrauskas published HRR curves from various transport vehicles and components [7]. The latest work is in the Handbook of Tunnel Fire Safety [8], the chapter on Heat Release Rates in Tunnel Fires: A Summary, authored by Ingason and Lönnermark in 2012 [9]. These summary works are largely reflected here and have been updated by the latest research.

The HRR during tunnel tests can be determined by different measuring techniques. The most common way is by using oxygen consumption calorimetry. The HRR can also be determined by measuring the weight loss of the fuel, the convective flow, or by using carbon dioxide generation calorimetry. The accuracy of these methods strongly depends on the measuring technique and the number and type of probes used. The calculation method also plays an important role but not as important as the technique used to determine the HRR.

Experience has shown that the total accuracy of HRR measurements in tunnel fires varies [10–12].The measurement error is on the order of 15–25 % in large-scale testing whereas in fire laboratories it is in the order of 7–11 %[13]. Ingason et al. [14] estimated the maximum error in their measurements in the EUREKA EU 499 testseries (FIRETUN) [15, 16] to be approximately 25 % (relative errors conservatively added), whereas in the Runehamar tests Ingason and Lönnermark [17] estimated the error to be 14.9 % (combined expanded relative standard uncertainty with a 95 % confidence interval [13]).This shows that the HRR measurements in tunnels yield relatively high uncertainty in the measured values.

In Chap. 3, the maximum or peak HRR values were presented for each large-scale test program, but in the following sections measured HRR are given for each type of vehicle or fuel, both as table values and in graphs.

4.2 Measured HRR in Different Vehicles

4.2.1 Road Vehicles

In Table 4.1, a summary of HRR measurements of passenger cars and other road vehicles is given [9]. For each test, an estimate of total calorific content, the measured peak-HRR and time to peak-HRR is given. In Table 4.1, the passenger cars have

Table 4.1 Large-scale experimental data on passenger cars [9]

Type of vehicle, model year, test nr, u=longitudinal ventilation m/s	Tunnel(T))/ Calorimeter C)	Tunnel cross-section (m^2)	Calorific content[b](GJ)	Peak HRR(MW)	Time to peak HRR (min)	Reference
Single passenger cars						
Ford Taunus 1.6, late 70's, test 1, NV	C		4	1.5	12	[19]
Datsun 160 J Sedan, late 70's, test 2, NV	C		4	1.8	10	
Datsun 180 B Sedan,late 70's, test 3, NV	C		4	2	14	
Fiat 127, late 70's, u=0.1 m/s	T	8	NA	3.6	12	[21]
Renault espaceJ11-II, 1988, test 20, u=0.5 m/s	T	30	7	6	8	[12]
CitroënBX,1986, NV[c]	C		5	4.3	15	[22]
Austin Maestro, 1982[c]	C		4	8.5	16	
Opel Kadett, 1990, test 6, u=1.5 m/s	T	50	NA	4.9	11	[23]
Opel Kadett, 1990, test 7, u=6 m/s	T	50	NA	4.8	38	
Renault 5,80's, test 3, NV	C		2.1	3.5	10	[24]
Renault 18, 80's, test 4, NV	C		3.1	2.1	29	
Small Car[a], 1995, test 8, NV	C		4.1	4.1	26	
Large car[a], 1995,test 7, NV	C		6.7	8.3	25	
Trabant, test 1, NV	C		3.1	3.7	11	[20]
Austin, test 2, NV	C		3.2	1.7	27	
Citroen, test 3, NV	C		8	4.6	17	
Citroen Jumper Van, test 11, u=1.6 m/s, sprinkler activated after 13.6 min	T	50	NA	7.6	NA	[23]
BRE test nr 7, NV	C		NA	4.8	45	[25]
BRE test nr 8, NV	C		NA	3.8	54	

Table 4.1 (continued)

Type of vehicle, model year, test nr, u=longitudinal ventilation m/s	Tunnel(T))/ Calorimeter C)	Tunnel cross-section (m^2)	Calorific content[b](GJ)	Peak HRR(MW)	Time to peak HRR (min)	Reference
Two passenger cars						
Citroen BX+Peugeot 305, 80's, test 6, NV	C		8.5	1.7	NA	[24]
Small car[a]+Large car[a], test 9, NV	C		7.9	7.5	13	
Large car[a]+Small car[a], test 10, NV	C		8.4	8.3	NA	
BMW+Renault 5, 80's, test 5, NV	C		NA	10	NA	
Polo+Trabant, test 6, NV	C		5.4	5.6	29	[20]
Peugeot+Trabant, test 5, NV	C		5.6	6.2	40	
Citroen+Trabant, test 7, NV	C		7.7	7.1	20	
Jetta+Ascona, test 8, NV	C		10	8.4	55	
BRE test nr 11 (stacked), NV	C		NA	8.5	12	[25]
Three passenger cars						
Golf+Trabant+Fiesta, test 4, NV	C		NA	8.9	33	[20]
BRE test nr 1, NV	C		NA	16	21	[25]
BREtest nr 2, NV	C		NA	7	55	
BREtest nr 3, NV	C		NA	11	10	

NA Not Available, *NV* Natural Ventilation

[a] Small Car (*SC*) includes the following cars: Peugeot 106, Renault Twingo-Clio, Citroen Saxo, Ford Fiesta, Opel Corsa, Fiat Punto, and WW Polo. Large Car (*LC*) includes the following cars: Peugeot 406, Renault Laguna, Citroen Xantia, Ford Mondeo, Opel Vectra, Fiat Tempra, and WW Passat

[b] Either based on integration of the HRR curve or estimation of fuel mass and heat of combustion. The error is estimated to be less than 25 %

[c] Cars burned in an approximate mockup of a Channel Tunnel shuttle wagon with a calorimeter hood/duct at each end

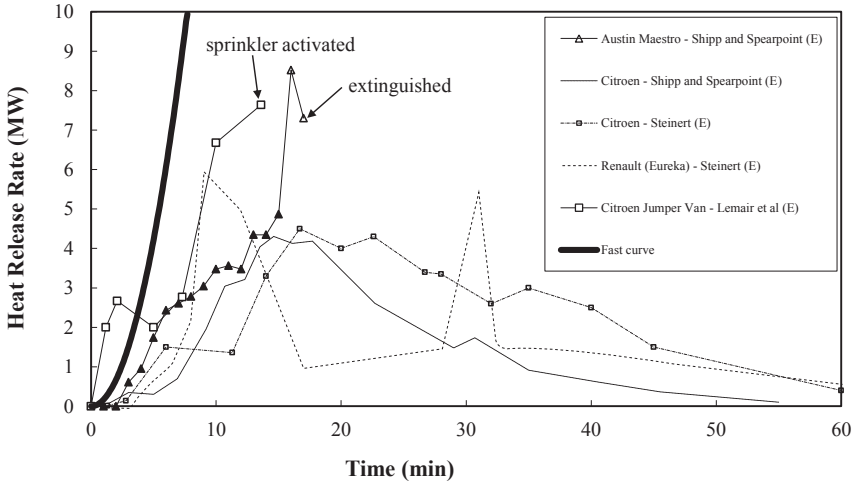

Fig. 4.1 Experimentally determined HRRs for single vehicle fires (passenger cars) [9]. Most of the data are extracted (*E*) from graphs found in the literature. If measured data are given it is indicated with (*M*). The references and more information are given in Table 4.1

either been burned under a calorimeter hood (C) or inside a tunnel (T), whereas all the large vehicles have been burned in tunnels.

4.2.1.1 Passenger Cars

HRRs in passenger cars are the most frequently obtained data found in the literature. Table 4.1 is essentially identical to the one given by Ingason and Lönnermark [9].

In Figs. 4.1 and 4.2 selected graphs of measured HRRs from single passenger cars are given. Most of these data are extracted from graphs given in each reference. For comparison, the t-squared fast fire growth curve [18] is also presented. In the following text, a short discussion of these tests is given.

HRRs from three full-scale laboratory tests using typical passenger cars (steel body) manufactured in the late 1970s (Car1, Car2, Car3) were presented by Mangs and Keski–Rahkonen [19]. The experiments were performed indoors using an oxygen calorimetry hood. Ignition was either inside the passenger cabin using a 0.09 m^2 heptane tray under the left front seat in test one or beneath the engine with an open 0.09 m^2 heptane tray yielding about 160 kW. The peak HRR ranged from 1.5–2 MW and the time to peak HRR varied from 10–14 min.

HRR of a plastic passenger car from a test in the EUREKA 499 test series [15, 16] was presented by Steinert [12]. The car used was a Renault Espace J11-II (1988) and was ignited in a transistor in the console in order to simulate a fire in the cable system. The peak HRR was 6 MW after 8 min.

HRRs of different types of passenger cars in a carpark, all with different types of car bodies (plastic and steel) have also been presented by Steinert [20]. The peak

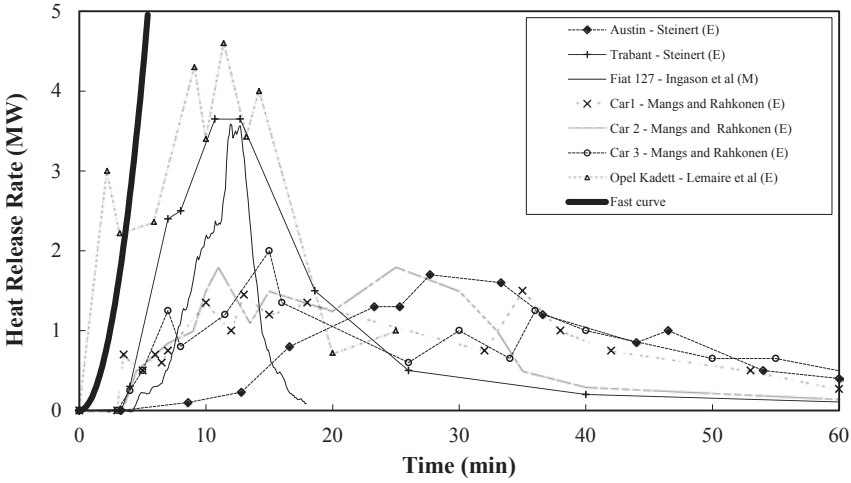

Fig. 4.2 Experimentally determined HRRs for single vehicle fires (passenger cars) [9]. Most of the data are extracted (*E*) from graphs found in the literature. If measured data are given it is indicated with (*M*). The references and more information are given in Table 4.1

HRR for single burning vehicles varied between 1.7–4.6 MW, acheived within the time frame of 11–27 min. A total of ten tests were performed in a carpark where the aim was to measure the HRR and quantify the risk for fire spread. The first three tests were carried out with single vehicles whereas the other six tests consisted of combinations of two and three passenger cars which were placed beside the ignited vehicle. The cars were ignited by dripping flammable liquid on the front seat with the front seat side window open. The peak HRR in the tests with two cars or three cars, presented by Steinert [20], varied between 5.6–8.9 MW and was achieved within the time frame of 20–55 min.

The HRRs for a 1982 Austin Maestro and a 1986 Citroën BX reported by Shipp and Spearpoint [22] are given in Fig. 4.1. The CitroënBX was ignited in the engine compartment with a small petrol pool fire of 5 kW. The Austin Maestro was ignited in the driver seat with a small wood crib of 10 kW. The test was carried out by using a calorimeter hood at each end of a canopy which was 8.7 m long and 3.5 m wide. The test setup was intended to represent a Channel Tunnel shuttle wagon. The peak HRR measured for the Citroën and the Austin Maestro was 4.3 and 8.5 MW, achieved after 15 and 16 min, respectively.

HRR measurements were presented by Lemair [23] for two Opel Kadetts (1990) performed with two different ventilation rates; 0 and 6 m/s, respectively. The fuel tank was filled with 25–30 l of petrol and the results are presented in Fig. 4.2. The peak HRR measured with no ventilation was 4.7 MW after 11.5 min, and with 6 m/s ventilation it was obtained in two steps: the first maximum was about 3 MW after 13 min, and the second one about 4.6 MW after 37 min. The high ventilation rate made it difficult for the fire to spread within the cabin in the opposite direction to

the ventilation flow. A test with a Citroen Jumper van was carried out during a test with a deluge sprinkler system in the tunnel ceiling. The sprinkler system was activated after about 13.6 min, see Fig. 4.1. Ingason et al. [21] presented HRR measurements for a Fiat 127 which was ignited in the engine compartment with an electrical device. The peak HRR was 3.6 MW after 12 min. The fire was extinguished by firefighters 13 min into the test, see Fig. 4.2.

Ten HRR measurements from passenger vehicle fires in a simulated carpark were presented by Joyeux [24]. Tests with one car and with two cars were carried out beneath a 10 MW calorimeter. Mazda, Renault, BMW, Citröen BX, and Peugeot, manufactured in the 1980s and 1990s, were used in the tests. The location of the ignition source was varied. In the first seven tests, the first car was ignited with a small petrol tray under the left front seat. In the other tests, the first car was ignited by a petrol tray placed under the car at gear box level. As can be seen in Table 4.1, the HRRs for single car fires (small and large passenger cars) varied from 1.5 to about 9 MW, but the majority of the tests show HRR values less than 5 MW. In the cases when two cars were involved the peak HRR varies between 3.5 and 10 MW.

Tests with passenger cars in a car park environment were presented by Shipp et al. [25]. Both single cars (BRE test nr. 7–8) and multiple cars (BRE test nr. 1–3) that were located side by side or stacked on each other were burned. The aim was to examine the time to reach a fully developed fire. The HRR of a fire starting in the passenger compartment or in the engine compartment of one of the vehicles was measured. The risk for fire spread from car to car was also documented. The results are only available in Table 4.1 and are indicated as BRE where BRE stands for British Research Establishment. The peak HRR for the two single vehicle tests was 3.8 and 4.8 MW after 54 and 45 min, respectively. With multiple vehicles it varied from 7–16 MW, occurring within a time frame of 10–55 min.

As the information on HRR in passenger cars is quite broad, it is possible to summarize it in a graph. In Fig. 4.3, a summary of the peak HRR data found for passenger cars is plotted as function of the time to peak HRR. It shows that the peak HRR for single vehicle fires (passenger cars) can vary from 1.5–8 MW, where most are lower than 5 MW. There are numerous test results available for two- and three-vehicle fires (passenger cars), although most of them are carried out in car parks and not tunnels. The variation in HRR for two-vehicle fires is 5.6–10 MW, and for three-vehicle fires it varies from 7–16 MW. The vast majority of tests show peak HHRs less than 10 MW, but one should bear in mind that these tests are mostly carried out in car parks, where very little longitudinal ventilation exists. Increased longitudinal ventilation may increase the fire spread between multiple vehicles, and thereby increase the peak HRR slightly.

The time to peak HRR varies between 8 and 55 min for single cars. In many of these tests, the peak occurs very late, depending on how the windows broke and which ventilation conditions were dominant. As indicated in Fig. 4.3 there is no clear correlation between the peak HRR and the time to achieve the peak HRR.

In over 80 % of the cases for single cars, the peak occurs within 8–30 min and for 60 % of the cases the peak occurs within 8–20 min. For two and three cars this

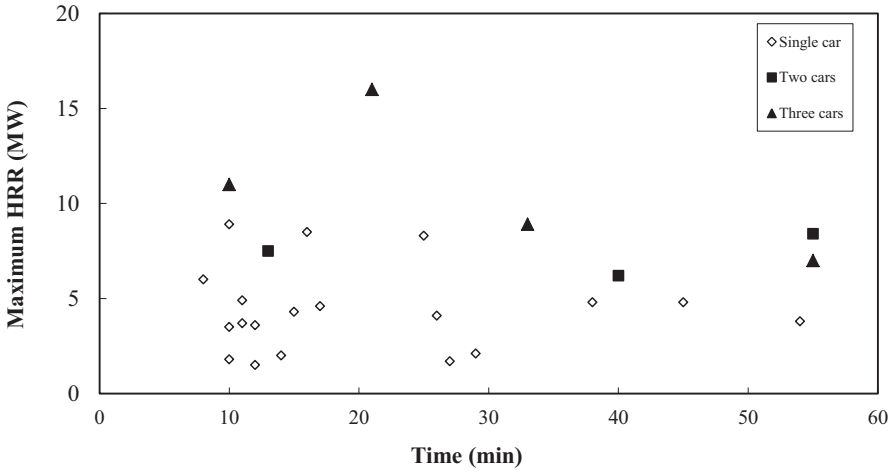

Fig. 4.3 Summary of time to reach peak HRR versus peak HRR for single, two- and three-vehicle fires (passenger cars)

time is more evenly distributed over the entire time spectra. In 95 % of the cases the HRR is less than 10 MW.

The experiments carried out by Joyeux [24, 26] indicated an increase in peak HRR for modern cars at the same time as the total energy content (GJ) was increasing. Ingason [3] analyzed the data and observed a tendency that peak HRR increased linearly with total calorific value (GJ) of the passenger cars involved. An analysis of all data available at that time showed that the average increase was about 0.7 MW/GJ. Lönnermark [27] did similar analysis for passenger cars and found out that the linear relationship between the peak HRR and the total energy content was 0.868 MW/GJ with a correlation coefficient R equal to 0.840.

4.2.1.2 Buses

There are not many large-scale tests with buses available. Only three tests which are relevant to this chapter are found in the literature. Details of these tests are provided in Table 4.2.

Ingason et al. [14] and Steinert [12] presented a measured HRR for a 12-m long Volvo school bus built in the 1960s made of fiberglass (EUREKA Bus, test 7). In the analysis of the HRR data, Steinert [12] used more coarse measurement points than Ingason et al. [14]. In Fig. 4.4 calculated values for the HRR of the test are given.

The peak HRR was measured to be 29 MW by Ingason et al. and 34 MW by Steinert. The total calorific content was estimated to be 41 GJ by Ingason et al. and 44 GJ by Steinert. The estimated time to peak HRR was 8 and 14 min, respectively.

In 2008, Axelsson et al. [28] carried out a large-scale experiment with a modern coach (Volvo manufactured in early 2000 with 49 seats). The test was conducted un-

Table 4.2 Large-scale experimental data on buses [9]

Type of vehicle, model year, test nr, *u*=longitudinal ventilation m/s	Tunnel (T)/Calorimeter (C)/Weightloss (W)	Tunnel cross-section (m^2)	Calorific content[d](GJ)	Peak HRR(MW)	Time to peak HRR (min)	Reference
Buses						
A 25–35 year old 12 m long Volvo school bus with 40 seats, EUREKA 499, test 7[a], u=0.3 m/s	T	30	41	29	8	[14]
A 25–35 year old 12 m long Volvo school bus with 40 seats, EUREKA 499, test 7[a], *u*=0.3 m/s	T	30	44	34	14	[12]
SP laboratory test with a modern tourist bus (Volvo), NV	C		NA	25[b)]	NA	[28]
A bus test in the Shimizu Tunnel, *u*=3–4 m/s	T	115	NA	30[c)]	7	[29]

NA Not Available, *NV* Natural Ventilation

[a] The test number sequence in the EUREKA 499 project is given in reference [30] and Table 3.5

[b] This value is based on estimation made by the authors of the report [28]

[c] This is estimated from the convective HRR of 20 MW derived by Kunikane et al [29] because a sprinkler system was activated when the convective HRR was 16.5 MW. We assume that 67% of the HRR is convective and thereby we can estimate the HRR=20/0.67=30 MW

[d] Based on integration of the HRR curve

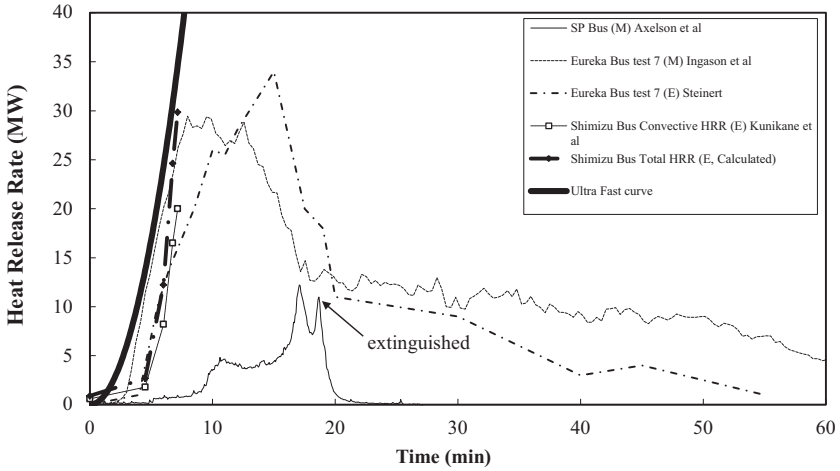

Fig. 4.4 HRRs for buses. More information about each test is given in Table 4.2 [9]. Most of the data are extracted (E) from graphs found in the literature. If measured data are given it is indicated with (M).

der a large hood calorimeter (nominal 10 MW capacity) inside a fire laboratory. The measured HRR is shown in Fig. 4.4. A t-squared ultrafast fire growth curve [18] is included for comparison. It is reported that the initial fire development was relatively slow. The fire was ignited with a 100 kW gas burner in the luggage compartment at the back of the bus and below the passenger compartment. The fire spread from the luggage compartment into the passenger compartment through the side windows. The fire started to grow significantly when three side windows in the passenger compartment had broken about 15–16 min after ignition. There are three peaks in the HRR curve given in Fig. 4.4. The first peak occurred after about 11 min, when the fire broke out on the side of the luggage compartment. The fire then spread into the passenger compartment through the windows between15–17 min after ignition. The situation in the fire laboratory became intolerable soon after that and the fire was extinguished manually at approximately 18.5 min after ignition (the last peak of the curve). There were problems with a leakage of heat and smoke as the hood collector did not have enough capacity during this period. The final HRR was probably higher than the measured peak shown in Fig. 4.4. The authors of the report estimated that the peak HRR could have been as high as 25 MW had the bus continued to burn.

The third test presented here was conducted in the Shimizu Tunnel in Japan. Part of the test was to examine the use of a sprinkler system [29], or a fixed firefighting system (FFFS), in road tunnels. The HRR was not measured but Kunikane et al. [29] estimated the convective peak HRR based on temperature measurements and the mass flow rate prior to the activation of the water spray system to be 16.5 MW. Kunikane et al. estimated that the peak convective HRR would have been approximately 20 MW if the FFFS had not been activated. Ingason [9] estimated the peak

HRR to be 30 MW by assuming that 67% of the total HRR is convective. Two HRR curves have been plotted in Fig. 4.4, one by extracting the information from Kunikane et al. [29] based on the convective HRR, and one showing the total HRR based on the assumption that 67% of the total HRR is convective.

4.2.1.3 Heavy Goods Vehicles

Most heavy goods vehicles (HGV) tests that have been carried out in tunnels use a mock-up simulating the cargo of a HGV trailer. Only those tests that are found in the literature and can be regarded as a free burning test, that is, without any interaction of a FFFS, such as sprinkler systems, are considered in this section. The peak HRR, fuel load and time to reach peak HRR are given in Table 4.3 and the HRRs are plotted in Fig. 4.5 and 4.6.

The first tests known as a HGV test was performed in 1992 in the EUREKA 499 test programme in Repparfjord in Norway [15]. A simulated HGV-trailer load (mock-up) was used, consisting of densely packed wood cribs supplemented by rubber tyres and plastic materials on the top (64 GJ). In this test, a natural ventilation rate of 0.7 m/s was obtained. The second test performed, also as a part of the EUREKA 499 test programme, was a fully equipped HGV truck and trailer loaded with mixed furniture (87 GJ) with varying longitudinal velocity during the test: 5–6 and 2–3 m/s. The peak HRR obtained was 23 MW after 15 min for the mock-up and 128 MW after 18 min for the real HGV.

A HGV test series was performed in the Mont Blanc tunnel in 2000 [31], with a HGV (truck and a trailer) similar to that which generated the fire in 1999 but with a much smaller amount of transported goods (35 instead of 76 GJ) [32, 31]. The fire load in the trailer consisted of 400 kg of margarine. The peak HRR of 23 MW was obtained after 47.5 min.

Another test series using HGV mock-ups was performed in the Second Benelux tunnel [23] in the Netherlands in 2001.Standardized wood pallets were arranged in two different configurations (approximately 10 and 20 GJ) with different longitudinal velocities: natural ventilation (~0.5 m/s), 4–5, and 5 m/s. The peak HRRs obtained were 13, 19, and 16 MW, respectively. The corresponding times were 16, 8, and 8 min.

A free burn test series was carried out in the Runehamar tunnel [17] in 2003. Four large-scale tests, each with a mockup of a HGV-trailer, which consisted of a steel rack system loaded with mixed commodities. The first test consisted of wood pallets and polyethylene pallets (Test T1), then wood pallets and polyurethane mattresses (Test T2), followed by furniture and fixtures with ten truck rubber tyres (Test T3), and finally paper cartons and polystyrene cups (Test T4).The commodity was covered with a polyester tarpaulin in each test and ignited on the upstream, front end, of the trailer. Initial longitudinal ventilation rates within the tunnel were in the range of 2.8–3.2 m/s. Peak HRRs measured were in the range of 66–202 MW. The peak HRRs were obtained between 7.1 and 18.4 min from ignition in the various tests.

Table 4.3 Large-scale experimental data on HGVs [9]

Type of vehicle, model year, test nr, u = longitudinal ventilation m/s	Tunnel (T)/Calorimeter (C)/Weight (W)	Tunnel cross-section (m^2)	Calorific content[d](GJ)	Peak HRR(MW)	Time to peak (min)	Reference
A simulated trailer load with total 11010 kg wood (82%[a]) and plastic pallets (18%), Runehamar test series, T1, u=3 m/s	T	32	240	202	18	[17]
A simulated trailer load with total 6930 kg wood pallets(82%[a]) and PUR mattresses (18%), Runehamar test series, T2, u=3 m/s	T	32	129	157	14	[17]
A Leyland DAF 310ATi—HGV trailer with 2 t of furniture, EUREKA 499, test 21, u=3–6 m/s	T	30	87	128	18	[36]
A simulated trailer with 8550 kg furniture, fixtures and rubber tyres, Runehamar test series, T3, u=3 m/s	T	32	152	119	10	[17]
A simulated trailer mockup with 2850 kg corrugated paper cartons filled with plastic cups (19%[a]), Runehamar test series, T4, u=3 m/s	T	32	67	67	14	[17]
A simulated trailer load with 72 wood pallets, Second Benelux tests, Test 14, u=1–2 m/s	T	50	19	26	12	[23]
A simulated trailer load with 36 wood pallets, Second Benelux tests, Test 8, 9 and 10, u=1.5, 5.3 and 5 m/s, respectively	T	50	10	13, 19 and 16	16, 8 and 8	[23]
A Simulated Truck Load (STL), EUREKA 499,test 15, u=0.7 m/s	T	30	63	17	15	[10]
Mont Blanc HGV mock up test	T	50	35	23	47.5	[31, 32]
A 3.49 t pickup truck loaded with 890 kg wood pallets; ignition in cargo, NV	W		26[b]	24[c)]	6.6	[37]

Table 4.3 (continued)

Type of vehicle, model year, test nr, u = longitudinal ventilation m/s	Tunnel (T)/Calorimeter (C)/Weight (W)	Tunnel cross-section (m^2)	Calorific content[d](GJ)	Peak HRR(MW)	Time to peak (min)	Reference
A 3.49 t pickup truck loaded with 890 kg wood pallets; ignition in cargo, NV	W		26[b]	21[c]	14.5	[37]
A 3.49 t pickup truck loaded with 452 kg plastic barrels; ignition of the seat, NV	W		25[d]	47[e]	43.8	[37]
Singapore—A test mock up consisting of wood and plastic pallets in a FFFS test	T	37.4		155	14	[33]
441 wood pallets in FFFS tests Runehamar	T	47	189	79	38	[35]

NA Not Available, *NV* Natural Ventilation

[a] Mass ratio of the total weight

[b] Estimated from the information given in the reference

[c] Given in the reference based on load cell measurements

[d] Either based on integration of the HRR curve or estimation of fuel mass and heat of combustion. The accuracy of these values may vary depending on the method and available information. The error is estimated to be less than 25%

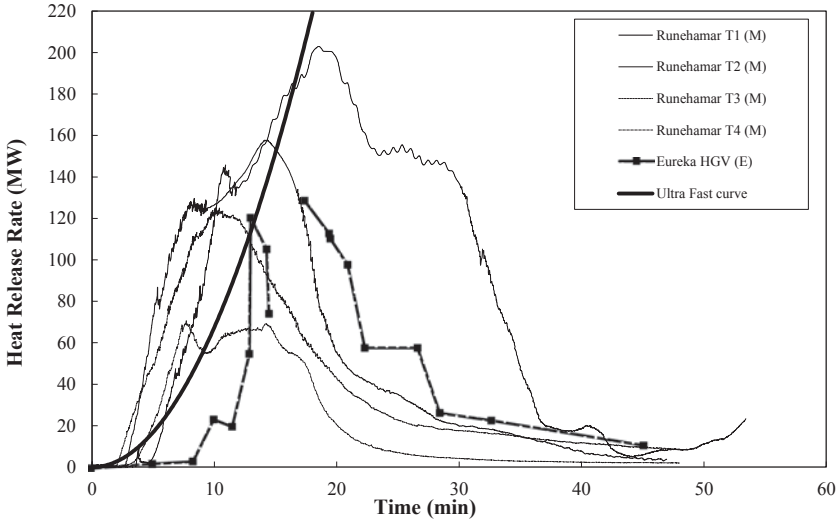

Fig. 4.5 The HRR for the HGV trailer mock-up tests presented in Table 4.3 [9]. (The EUREKA HGV test number 21 was for a real HGV, including the cab) [9].Most of the data are extracted (*E*) from graphs found in the literature. If measured data are given it is indicated with (*M*)

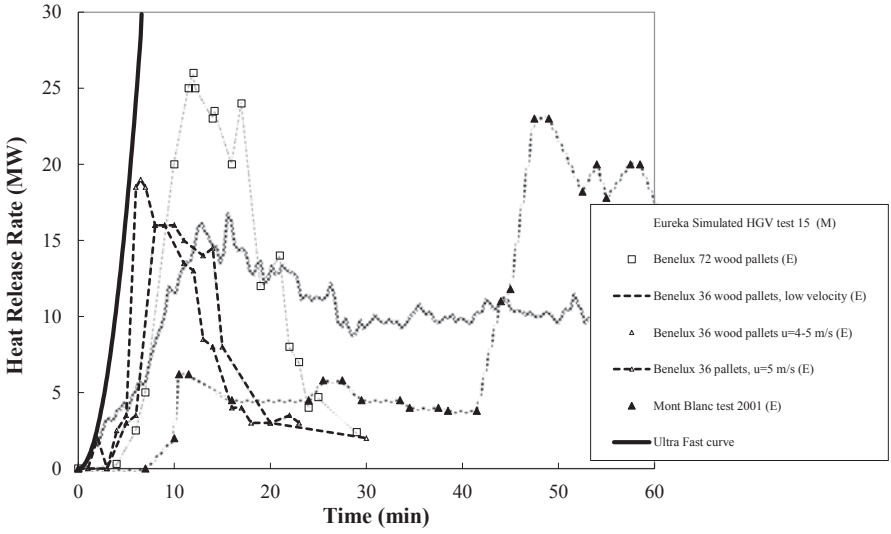

Fig. 4.6 The HRR for the HGV trailer mock-up tests presented in Table 4.3 [9].Most of the data are extracted (E) from graphs found in the literature. If measured data are given it is indicated with (M).

Since 2003, numerous large-scale tests with focus on testing FFFS have been performed. Most of them do not include a free burn test, and they are presented in more detail in Chap. 16. There are at least two test series that included at least one free burn test, namely a test in the Singapore programme with wood pallets and plastic pallets [33, 34]. Also, in 2013 fire tests with 441 wood pallets (420 main fire load and 21 in a target (a pile of wood pallet used to investigate plausible fire spread) were performed in the Runehamar tunnel [35].

The variation in the peak HRRs for HGVs are from 13–202 MW. The Runehamar test results in 2003 varied from 67–202 MW. One should bear in mind that nearly all the HGV tests (except the 120 MW EUREKA test that included a furniture load and a truck cabin where the fire was ignited inside) were carried out as a piled commodity on an elevated platform, with a minimum of containment of the fire load. In most cases a plastic tarpaulin covered the piled commodity and burned very fast without spreading the fire. The ignition source was also placed inside the commodity, usually on the upstream side. Initially the tarpaulin delayed the fire spread mainly due to wind protection, but as soon as it burned off, the wind affected the fire spread by deflecting the flames. The deflection of the flames throughout the cargo is the most important parameter for fast fire growth rates in this type of test mock-up. Any type of wind protection delayed the fire growth considerably. This is discussed in more detail in the fire growth rate Chap. 5.

These are all factors that may affect the initial fire growth rate in comparison to a fire in a real HGV. The peak HRR values, however, depend more on the amount of exposed fuel surface area (the way it is piled) and the ventilation conditions in close proximity to the fuel load (shielding effects, containment, etc.). This means that the way the commodity is piled or stored is an important factor to consider. If the cargo is relatively open it is possible to calculate the peak HRR based on exposed fuel surface area.

If the cargo is enclosed within a steel container or other time delaying material the fire development may be different compared to the values presented here. The effect of the tunnel geometry (especially the tunnel height) is also an important issue as the fire load interacts with its physical environment when it is burning.

In Fig. 4.7 a plot of the HRR versus time to reach a peak value is shown for all available experiments with HGV fire loads. It shows that the time to reach peak HRR is between 8–18 min and the peak HRR varies between 13–202 MWs.

Lönnermark [27] analyzed the correlation between the peak HRR and the total energy content of HGVs. There was a scatter in the data and there were differences in test conditions, but he concluded that there is a clear relationship between the peak HRR and the energy content using 0.866 MW/GJ ($R=0.910$).Later, Kashef et al. [38] examined the tests data from 2nd Benelux tunnel, EUREKA 499 tests and from the Runehamar tests, and showed that the peak HRR correlates with the released total energy for well ventilated fire using 0.9 MW/GJ. Although the existence of this good correlation, one should be careful in using them. There is no physical evidence for this correlation except that higher the total energy content is larger volume of combustible material is expected. The larger the volume or weight of material is in place, often the larger the exposed fuel surface area is. However,

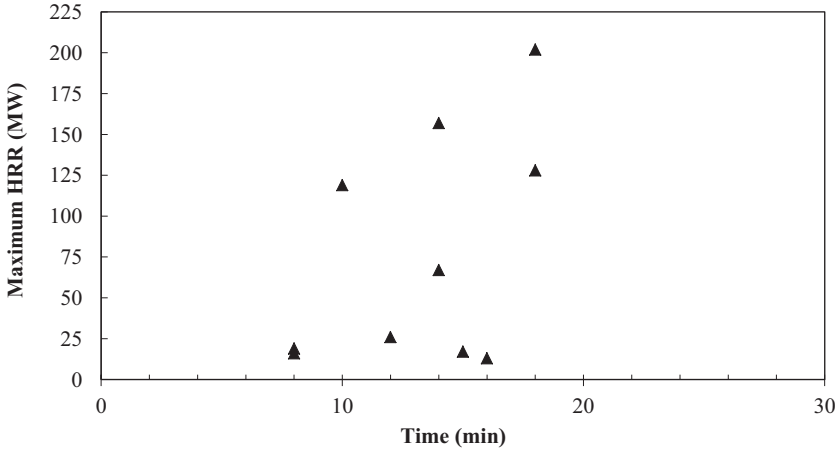

Fig. 4.7 Summary of time to reach peak HRR versus peak HRR for HGV fire loads

this does not always have to be true. It is more related to how the goods are stored, rather than how much volume or weight is in place. Larger exposed surface areas, for the same weight or volume of material, increase the peak HRR.

4.2.1.4 Tanker Fires

A full scale tanker test in a tunnel has never been reported. All the values found in the literature or in standards are based on estimates. These estimates show HRR values varying between 10–400 MW. These values are dependent on the initial type of accident, leakage flow, the way the gasoline or diesel is contained etc. The tank material (aluminium or steel) has a major effect on the result as well as the position of the vehicle (turn over, crash, etc.) in relation to the initial fire. Although there are no large-scale results reported on HRR tests using gasoline or diesel tankers found in the literature, there are numerous tests that have been carried out using pool fires, see Sect. 4.2.1.5.

The fire size of burning road gasoline tankers in tunnels reported in the literature are usually based on a possible spillage size and no concern is given to the road tanker itself containing a volume of liquid inside a tank. Heselden [39] assumed a gasoline fire to produce about 2 MW/m^2 (pool fire) and following Heselden proposal, Liew et al. [40] assumed a spillage area from a leaking tanker to be 50 m^2 thus producing a 100 MW fire.

Very few road gasoline tanker accidents in tunnels leading to fire have occurred in the world. The road tanker accident in the Caldecott tunnel in the USA in 1982, where a gasoline trailer collided and overturned, is the best source available today [41, 42]. Larson et al. [41] carried out a thorough analysis of the gasoline tanker accident in the Caldecott tunnel (USA 1982) showing that about 33 300 L gasoline

was burned within 40 min. Hence the average burning rate would be 14 L/s which yield about 430 MW fire assuming complete combustion. However, in tunnels complete combustion is usually not achieved for such large fires without a high velocity longitudinal ventilation system. An estimate given by Ingason indicates that the Caldecott tanker fire HRR was probably less than 300 MW [43]. The knowledge about the effects of ventilation on combustion efficiency in such large fires is not clearly known.

Ingason [43] describes how the HRR from a road gasoline tanker accident was estimated with aid of small-scale testing together with a theoretical calculation and analysis of an actual road tanker accident such as the Caldecott tanker fire. For the case studied, the initial spillage fire HRR caused by a collision can be in the range of 10–300 MW. This range includes small spillage fires created by small leaks where the entire spill burns up before it reaches the drainage system to large spillage fires creating a bulk tank fire where the tank is engulfed in flames. In the case of an aluminum road tanker, the initial spillage fire can eventually lead to a bulk tank fire since, the top of the tanks may open up. The unwetted walls will gradually disappear because aluminum parts will soften and fall into the tank and because parts will melt. The burning rate per square metre fuel surface could become more than five times higher than ordinary pool fires since, the gasoline bulk starts to boil after some time. Depending on the combustion efficiency the aluminum bulk tank fire HRR can be in the range of 200–300 MW and for the case studied the fire duration can be in the range of 50–60 min. Good agreement is found between the theoretically calculated burning rates and experimentally determined values for a bulk tank fire using model scale experiments [43]. As pool fires usually constitute the basis for estimation of tanker fire size, a more thorough analysis of such fires is given in Sect. 4.2.2.5.

4.2.1.5 Pool Fires (Liquid)

Babrauskas [44] presented numerous data on liquid pool fires that can be compared to the tests carried out in tunnels. Babrauskas [44] has also used the following equation, which was originally given by Zabetakis and Burgess [45] to calculate the HRR for pool fires:

$$\dot{q}'' = \dot{m}''_{\infty}(1 - e^{-k\beta D})\,\chi \Delta H_c \cdot A_f \tag{4.1}$$

where $\dot{m}''_{\infty}$ is the highest value for mass burning rate (kg/(m^2 s)) obtained from tabulated data for each fuel in Babrauskas [44] (in Table 3–1.13), D is the pool diameter (m), ΔH_c is the effective heat of combustion (MJ/kg), χ is the combustion efficiency, A_f is the pool area (m^2) and $k\beta$ is the product of the extinction–absorption coefficient of the flame k (1/m) and the mean bean-beam-length corrector β. The product $k\beta$ has the dimension (m^{-1}).Values for petroleum products from Table 3–1.13 in Babrauskas [44] are reproduced in Table 4.4, in order to be used later in tables and examples.

Table 4.4 Empirical constants for use in Eq. (4.1). Values reproduced for petroleum products from Table 3–1.13 in Babrauskas [44]

Material	Density (kg/m^3)	Heat of gasification L_g (KJ/kg)	Heat of combustion ΔH_c (MJ/kg)	Mass burning rate $\dot{m}''_\infty$ (kg/(m^2 s))	Empirical constant in Eq. (4.1) $k\beta$ (m^{-1})
Benzine	740	–	44.7	0.048	3.6
Gasoline	740	330	43.7	0.055	2.1
Kerosene	820	670	43.2	0.039	3.5
Jp-4	760		43.5	0.051	3.6
Jp-5	810	700	43.0	0.054	1.6
Transformer oil	760	–	46.4	0.039	0.7
Fuel oil	940–1000	–	39.7	0.035	1.7
Crude oil	830–880	–	42.5–42.7	0.022–0.045	2.8

Example 4.1 What is the HRR from a gasoline pan fire that is 1.5 m in diameter?

Solution: Use Eq. (4.1) and select corresponding values from Table 4.4. For gasoline $\dot{m}''_\infty = 0.055$ *kg/(m*^{2} *s),* $k\beta = 2.1$ *m*$^{-1}$, $\Delta H_{c,eff} = 43.7$ *MJ/kg (assuming* $\chi = 1$*) and the area is* $\pi x\ 1.5^2/4 = 0.56$ *m*^{2}*. The total HRR is* $0.055 \times (1 - e^{-2.1 \times 1.5}) \times 43.7 \times 0.56 = 1.3$ *MW or per fuel surface area* $\dot{q}'' = 1.3/0.56 = 2.3$ *MW/m*^{2}*.*

The HRR for different pool fire tests conducted in tunnels is presented in Table 4.5. The majority of the tests have been carried out using circular or square pans with relatively deep fuel depth, both with or without a water bed under the fuel. It is assumed that the depth of the fuel was more than 80 mm, and the minus sign (−) is given in cases where the fuel depth is uncertain or not reported. Tests with a fuel depth less than 80 mm are also presented in Table 4.5.

For comparison, values using Eq. (4.1) are given in Table 4.5. If no information is available for the fuel it does not appear in Table 4.5 and if the area A is not known, A is set equal to 1.0 m^2.

In the Ofenegg tests in 1965 [46] the influences of the ventilation conditions and the tunnel and fuel pan geometry on the burning rate were clearly demonstrated. The tunnel was only 190 m, with one portal (dead end tunnel). The distance from the portal to the nearest edge of the pans was 130 m. Three different types of ventilation conditions were possible to obtain in the test tunnel: natural ventilation, semi-transverse, and longitudinal ventilation.

In the case of natural ventilation one could expect that this is similar to an enclosure fire, that is, one opening at the portal. Estimation of the HRR using Eq. (4.1) yields a HRR of 84.5 MW. This is much higher than obtained in the natural ventilation tests for larger pans with A=47.5 and 95 m^2, or 35–39 MW (see Table 4.5). Even for the semi-transverse ventilation case the HRR was in the same range. The only explanation is the effect of inerting (vitiation) on the HRR, through mixing of combustion products with the incoming fresh air.

Table 4.5 Summary of pool fire tests in tunnels and laboratories

Fuel type	Test place/ ventilation (see Chap. 3 for more details about each test)	Fuel depth (mm)	Fuel area (m^2)	HRR (MW)	HRR per square metre fuel (MW/m^2)	Eq (4.1) HRR per square metre fuel (MW/m^2)
Gasoline	Ofenegg (test 1)—natural	–	6.6	16	2.4	2.4
	Offenegg (test 2)—semi-transverse	–	6.6	12	1.8	
	Offenegg (test 2a)-longitudinal	–	6.6	12	1.8	
	Offenegg (test 7a)—longitudinal	–	47.5	70	1.5	
	Offenegg (test 5)—natural	–	47.5	39	0.8	
	Offenegg (test 6)—semi-transvers	–	47.5	38	0.7	
	Offenegg (test 9)—natural	–	95	35	0.4	
	Offenegg (test 10)—semi-transverse	–	95	32	0.3	
	Zwenberg (test 101)	–	3.4	8	2.4	
	Zwenberg (test 210)	–	6.4	12	1.9	
	Zwenberg (test 301)	–	13.6	20	1.5	
	PWRI (test 1)	–	4.0	9.6	2.4	
	SP	50	2	5.8	2.9	2.4
	SP	7	2	4.5	1.6	
	SP	2–3	6	5	0.8	
Diesel	Zwenberg (test 220)	–	6.40	10	1.6	
	SP	–	2.8	3.5	1.3	1.6
	SP	20	1.2	1.8	1.5	
	SP	1–2	–	–	0.25–0.3	
Kerosene	SP	70	0.4	0.7	1.7	1.7
	Glasgow	–	–	–	1.4	
Heptane	EUREKA (test 16)	–	1.0	3.5	3.5	
	EUREKA (test 18)	–	3.0	7.0	2.3	

Table 4.5 (continued)

Fuel type	Test place/ ventilation (see Chap. 3 for more details about each test)	Fuel depth (mm)	Fuel area (m^2)	HRR (MW)	HRR per square metre fuel (MW/m^2)	Eq (4.1) HRR per square metre fuel (MW/m^2)
	SP	70	0.4	1.14	2.7	2.6
n-60 % heptane/40 % toluene	2nd Benelux (test 1)	–	3.6	4.10	1.1	
	2nd Benelux (test 2)	–	3.6	3.50	1.0	
	2nd Benelux (test 2)	–	7.2	11.5	1.6	
Low-sulfur No 2 fuel oil (diesel)	Memorial	–	4.5	10	2.2	
	Memorial	–	9.0	20	2.2	
	Memorial	–	22.2	50	2.3	
	Memorial	–	44.2	100	2.3	
JP-5	SP	5	2.8	4.8	1.7	
	SP	2.5	2.8	3.1	1.1	
	SP	1	2.8	1.1	0.4	

In the first test with natural ventilation, the average burning rate was 0.059 kg/(m^2 s) for a 6.6 m^2 fuel pan, that is, 2.4 MW/m^2. In the tests with semi-transverse and longitudinal ventilation and a 6.6 m^2 pan, the HRR per unit fuel area was reduced to 1.8 MW/m^2. In the tests with the 47.5 m^2 fuel pan the burning rate for natural and semi-transverse ventilation was 0.8 and 0.7 MW/m^2, respectively, whereas in the test with longitudinal ventilation the HRR is 1.5 MW/m^2. In the 95 m^2 pan the HRR per unit fuel area was only 0.3–0.4 MW/m^2 which corresponds to 83 % of the HRR per unit fuel area in the open.

It is evident that the HRR per unit fuel area and thereby the total HRR in these tests is highly influenced by ventilation and the test setup. The poor accessibility of oxygen to the fuel bed is the main reason [6] together with the fact that the Ofenegg tunnel was a ‘dead end’ tunnel. In the case when no mechanical ventilation was applied, the only air supply came from the portal on one side of the fire and therefore,one can expect effects of vitiation in the same way as described in Chap. 2, Sect. 2.6.

In the Zwenberg tests in Austria in 1974–1975 [47], the results were much more consistent with expectations in tunnel fires. The main reason is that the tunnel had two portals, which makes a huge difference in the way the air is supplied to the fire. Only mechanical ventilation was available (longitudinal, semi-transverse, and transverse ventilation). The average burning rate per square metre fuel area of gasoline for all the tests was 0.043 kg/(m^2 s) with a standard deviation of 0.0075 kg/(m^2 s). This corresponds to a HRR per unit fuel area of 1.9 MW/m^2, and standard

deviation of 0.3 MW/m^2. The average reduction in the burning rate was about 22 % of the HRR per fuel surface in the open.

Some tests with smaller fuel depths have been carried out by SP Technical Research Institute of Sweden (SP), but have not been reported earlier. In Table 4.5, tests with fuel depths less than10 mm, and tests with larger fuel depths are given. Most of them were conducted in a pan but the SP gasoline test of 2–3 mm consisted of continuous outflowing of 22 L/min of gasoline on a sloped concrete surface. The JP-5 tests with a small fuel depth were carried out on a water bed. It is clear from the results given in Table 4.5 that the fuel thickness is an important parameter to consider. The HRR per fuel surface area can be reduced by 70–80 % of the large fuel depth value if the fuel is only a few millimeters deep. A fuel on an asphalt road surface can be expected to be not more than a few millimeters thick. This has to be taken into account when considering the HRR from different pool fires on road surfaces.

In the cases where the ventilation did not have a large influence on the results, the calculated values in Table 4.5 show a very good correspondence with the values obtained from experiments with different types of pool fires.

Tests have been performed to study the influence of a layer of railway macadam on the HRR of a burning liquid spill [48]. The test shows that the presence of the macadam has a significant decreasing effect on the burning rate for the two fuels tested: heptane and diesel. The influence increases with the distance from the fuel surface to the upper layer of the macadam. This is discussed in more detail in Chap. 11 on fire spread.

4.2.1.6 Construction Vehicles

Vehicles used in the construction of tunnels are also presented here. Hansen and Ingason [49] presented large-scale tests of vehicles common in the mining industry. The tests were carried out in an underground mine in Sweden in 2011. The aim of the full-scale fire experiments was to determine the HRR because information was unavailable in the literature. This information is vital for fire safety engineers working in underground mines and tunnel construction sites. Two full-scale fire tests were carried out, one with a wheel loader and one with a drilling rig. Each of these vehicles had been in service for several years. The HRR results from the two vehicles tested are shown in Fig. 4.8.

The wheel loader was a Toro 501 DL and was diesel powered. The wheel loader was used for hauling iron ore between the production areas to a vertical shaft, where the iron ore was unloaded. The vehicle was 10.3 m long, 2.8 m wide and almost 3 m high. The total weight was 36 t. The fuel load consisted primarily of the four tyres. The tyre specification of 26.5 × 25 L5S implies a tyre with a section width of 26.5 in. (~ 0.66 m), a rim diameter of 25 in. (0.625 m) and with smooth extra deep tread. The total fire load of the wheel loader combustible components was estimated to be 76.2 GJ. The tyres of the wheel loader were filled with water (instead of air) due to the risk of tyre explosion during normal operation.

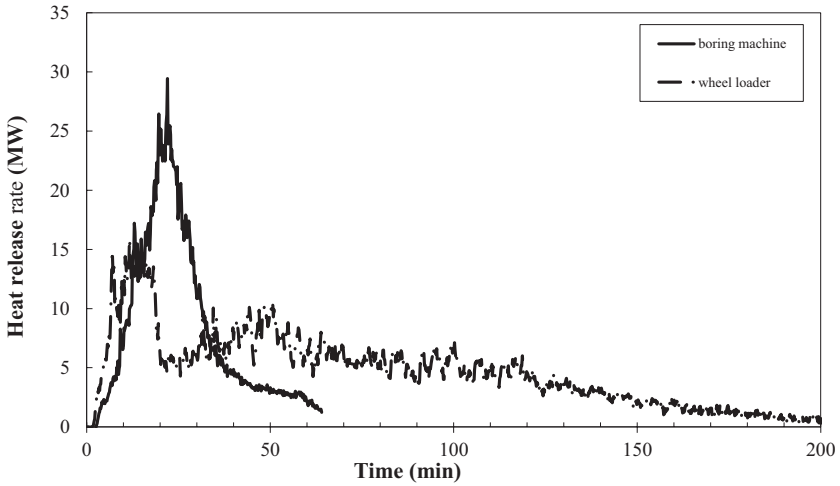

Fig. 4.8 A plot of HRR for a front wheel loader and a drilling machine [49]

The drilling rig was an Atlas Copco Rocket Boomer 322, which is an electrically driven vehicle commonly used in underground mines. The drilling rig was also equipped with a diesel powered engine which is used when moving the drilling rig from one site to another. The total length with boom was 12.4 m. The width was 2.2 m and the total height was about 3 m. The total weight was 18.4 t. The fuel load of the drilling rig consisted primarily of four tyres, the hydraulic oil and the hydraulic hoses. The tyre specification of 13.00 × 20 PR 18 implies a tyre with a section width of 13 in. (0.325 m) and a rim diameter of 20 in. (0.5 m).The combustible components were estimated to be 45.8 GJ.

In both tests, the ignition source consisted of a circular tray (1.1 m) that was placed under the fuel tank of each vehicle and located close to at least one tyre. The trays were filled with diesel fuel in order to simulate a pool fire caused by leaking diesel from the tank.

4.2.1.7 Rubber Tyres

As rubber tyres of large road or construction vehicles give an important contribution to the HRR, it is of interest to present some HRR results on rubber tyres.

Ingason and Hammarström [50] reported on a fire test with a front wheel loader rubber tyre under a large laboratory calorimeter. The test was carried out by igniting a pan with gravel and diesel placed under the tyre. The rubber tyre was a Good Year with the specification of 26.5R25 Tubeless. The total diameter of the tyre was 1.75 m and the total width (tread) was 0.67 m. The tread is the part of the tyre which

comes in contact with the road surface. The total external and exposed surface area of the rubber tyre was estimated to be about 8 m^2. The total weight, including the wheel rim, was 723 kg. A peak HRR of 3 MW after 90 min was recorded. It was also concluded that 86% of the total heat energy had been released 2.5 h after ignition.

In 1993, the BRE in the UK [51] conducted two large-scale tests on tyres under a large calorimeter at the Fire Research Station's Cardington Laboratory. In the first test, the tyres were stacked horizontally and in the second, vertically. In each test, a stack of eight tyres was burned and numerous measurements were made, among them the HRR. The tyres used were ordinary passenger car tyres without a steel rim. The vertical stacking (eight tyres high) produced a far more severe fire than the horizontally stacked tyres. The peak HRR was 1300 kW for the vertical stack and 500 kW for the horizontal stack. The reason for the difference was faster fire spread and better flow of air to the center of the tyres when stacked vertically compared to the horizontal stacking. In the horizontal case parts of the tyres that burned initially were burned out when the fire was terminated.

The Fire Laboratory of SINTEF in Norway presented in 1995 heat release data from two tests (A and B) with rubber tyres used for HGVs [52]. A pair of dual load bearing wheels was tested under a laboratory calorimeter. The ignition was simulated by heating the wheel rims. An insulated pipe was welded to the wheel rims and heated by a gas fire passing through the pipe. The metal wheel rim was heated to a temperature that ignited the rubber tyres. This procedure was continued for about 30 min prior to ignition. The size of the tyres varied, but in test A the tyre specification was 285/80 R22.5 and in Test B the tyre specification was 315/80 R22.5. This means that in test A the tyre was 285 mm wide with a 228 mm (0.8×285) high vertical surface and the rim diameter was 22.5 in. (575 mm). The exposed rubber area was estimated to be 4.2 m^2 for test A and 4.8 m^2 for test B (dual tyres) [50]. The measured maximum HRR for test A was 878 kW and for test B 964 kW. The time to attain the maximum HRR was 29 and 27 min, respectively, from ignition. The fire duration was about 60 min in both cases.

In 2005, Lönnermark and Blomqvist [53] carried out tests using ordinary passenger car rubber tyres and the peak HRR was recorded. The aim of the tests was to assess the emissions to air and water from a fire in tyres. Each test involved 32 passenger car tyres without a wheel rim. Two different storage setups were used: heaped and piled. Both setups represent common ways to store used tyres. The heap storage was more spread out. It had a base of 3×3 tyres, with the tyres stacked in a certain pattern above. The pile configuration consisted of a base with 2×2 tyres stacked on each other in a straight vertical pile. This means that there were eight tyres in each stack, that is, a total of 32 tyres. In both setups the tyres were placed on a steel pan, 2×2 m, under a large calorimeter. The tyres varied somewhat in size, but tyres that were as similar as possible were used. The maximum HRRs from the tests were as follows: heap storage—3.7, 3.6 and 3.7 MW; pile storage—3.6 MW. The maximum HRR in the pile storage test occurred 19 min after ignition.

4.2.2 Railway Rolling Stock

The literature describes very few measurements of HRR for rail and metro vehicles (rolling stock). The majority of the tests available are from the EUREKA 499 test series [15], but in recent years more test data have been published [54, 55]. In Table 4.6, a summary of available tests is given. For more information about each large-scale test, read Chap. 3.

The test results presented in Table 4.6 are based on tests with single coaches. The peak HRR is found to be in the range of 7–77 MW and the time to reach the peak HRR varies from 5–80 min. If the fire were to spread between the train coaches, the total HRR and the time to peak HRR would be much higher than the values given here although one cannot simply add the HRR for each coach to obtain an estimate of the total HRR because the first coach would not necessarily reach the peak HRR at the same time as the later ones. The EUREKA 499 tests show that there are many parameters that will affect the fire development in a train coach. These include the body type (steel, aluminum, etc.), the quality of the glazed windows, the size and geometry of the openings, the amount and type of combustible interior material and its initial moisture content, the construction of wagon joints, the air velocity within the tunnel and the geometry of the tunnel cross-section. These are all parameters which need to be considered in the design process of a rail or metro tunnel. A very important factor for the development of the fire is the quality and mounting of the windows. As long as the windows do not break or fall out (and there are no other large openings), the fire will develop slowly. On the other hand, if the windows break the fire can spread and intensify very quickly. In Fig. 4.9 time-resolved HRR curves are given for some of the tests presented in Table 4.6. For comparison, the t-squared ultrafast fire growth curve [18] is also included.

4.3 Parameters Influencing the HRR

The HRR can be affected by many parameters. This can be due to heat feedback from the tunnel construction, the ventilation conditions inside the tunnel and the geometry of the fuel. In the following text, a summary of these effects are presented.

4.3.1 Heat Feedback

When a vehicle fire occurs in a tunnel it communicates with its surrounding surface boundaries, hot smoky gases, and the surrounding flames through electromagnetic waves (radiation, see Chap. 10). The consequence will be a transient temperature increase of the tunnel structure surfaces. Depending on the type of lining or surface (rock, concrete, boards, etc.), the surface temperature will increase at different rates. The initial temperature of the surrounding surface can be very low, on the order of

Table 4.6 Large-scale experimental data on rolling stock [9]

Type of vehicle, test series, test nr, u = longitudinal ventilation m/s	Calorific content(GJ)	Peak HRR(MW)	Time to peak HRR (min)	Reference
Rail				
A joined railway car; two half cars, one of aluminium and one of steel, EUREKA 499, test 11, u=6–8/3–4 m/s	55	43	53	[12]
German IntercityExpress railway car (ICE), EUREKA 499, test 12, u=0.5 m/s	63	19	80	[14]
German Intercity passenger railway car (IC), EUREKA 499, test 13, u=0.5 m/s	77	13	25	[14]
British Rail 415, passenger railway car[a]	NA	16	NA	[56]
British Rail Sprinter, passenger railway car, fire retardant upholstered seatings[a]	NA	7	NA	[56]
Intercity train car (u=2.4 m/s) 37 m long tunnel Carleton laboratory facility	50	32	18	[55]
Metro				
German subway car, EUREKA 499, u=0.5 m/s	41	35	5	[14]
METRO test 2 (u=2–2.5 m/s)	64	76.7	12.7	[54]
METRO test 3 (u=2–2.5 m/s)	71	77.4	117.9	[54]
Subway car (u=2.4 m/s)37 m long enclosure Carleton laboratory facility	23	52.5	9	[55]

[a] The test report is confidential and no information is available on test setup, test procedure, measurement techniques, ventilation, etc.

5–10 ℃ for rock or concrete tunnels. In the vicinity of the fire, the flames radiate back toward the fuel surface, as well as outward to the surrounding surfaces and hot smoky gases. Depending on the ventilation conditions, a hot smoke layer is created above or downstream of the fire. This hot smoke layer interacts through radiation with the fuel source as well as the tunnel surfaces through convection and radiation. The outward radiated heat from the burning vehicle is partly reflected back from the tunnel surfaces and is partly absorbed, which will increase the surface temperature. Locally, above the fire, there is also a higher degree of exchange of convective heat to the tunnel surfaces. Gradually, the surrounding tunnel surfaces are heated up and the temperature rises continuously. At some point the surrounding surface become an important source of external radiation toward the burning fuel surface, especially in very large fires. This does not necessarily mean that the incident radiation toward

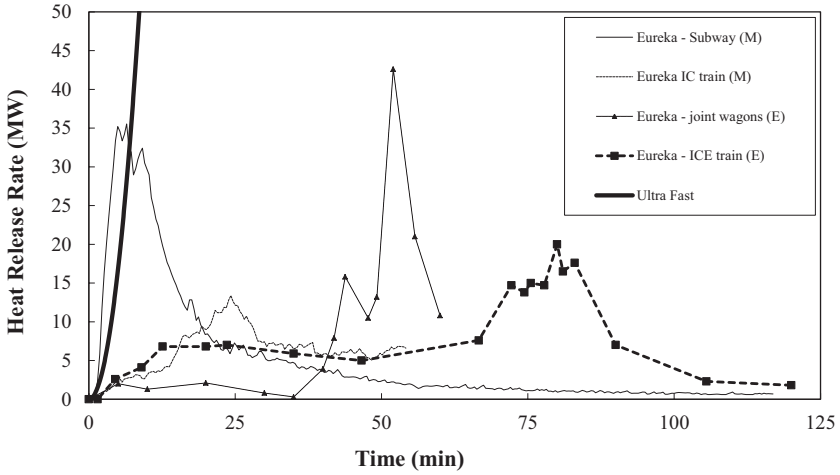

Fig. 4.9 The HRR for rail vehicle tests presented in Table 4.6 [9].Most of the data are extracted (*E*) from graphs found in the literature. If measured data are given it is indicated with (*M*)

the fuel surface is increasing continuously. The ceiling surface is usually covered by flames or black smoke, and therefore, a limited exchange of radiation with the fuel surface is obtained, and thereby the effects on the burning rate are indirect. The radiation from the ceiling surface is absorbed by the hot smoke gases and the flame volume, however, the side walls may have more direct interaction with the fuel surface. The extension of this interaction is dominated by view factors and the shielding effects within the fuel.

The HRR per square metre of a given fuel surface is given by the heat balance equation:

$$\dot{q}'' = (\dot{q}_f'' + \dot{q}_g'' + \dot{q}_w'' - \dot{q}_{rr}'')\frac{\Delta H_{c,eff}}{L_g} \tag{4.2}$$

where $\dot{q}''$ is the HRR per unit surface area (kW/m^2) of the fuel or vehicle, $\dot{q}_f''$ is the radiation from the flame volume toward the surface (kW/m^2), $\dot{q}_g''$ is the radiation from the hot smoke gases in the vicinity of the fire (kW/m^2), $\dot{q}_w''$ is the radiation from the surrounding walls and ceiling (kW/m^2) and $\dot{q}_{rr}''$ is the reradiation from the fuel surface (kW/m^2). In Fig. 4.10, the parameters in Eq. (4.2) are shown in a side perspective. $\dot{q}_g''$ can be written as $F_e\varepsilon_g\sigma T_g^4$ where T_g is the characteristic temperature of the smoke layer and $\dot{q}_w'' = F_w\varepsilon_w\sigma T_w^4$ where T_w the surface temperature of the surrounding tunnel structure (K). The view factor F can vary as well as the emissivity ε for the gas (index g) and the surface (index w). σ is the Stefan–Boltzmann constant 5.67×10^{-11} kW/(K^4 m^2).

The importance of each temperature term can vary spatially. In most cases it is dominated by T_g, but sometimes by T_w, especially if the side walls become warm. The surface temperature rise of the walls is time dependent, and varies for different

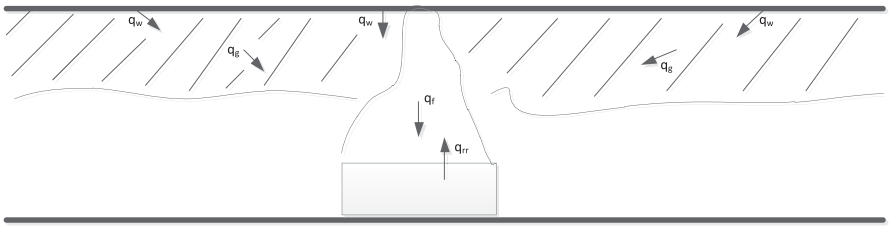

Fig. 4.10 An illustration of the terms used in Eq. (4.2)

materials. For example if a rock tunnel wall is suddenly exposed to 1000 °C, it will take about 6 min for the surface temperature to reach 80 % of the exposed gas temperature, and 20 min to reach 90 %. The corresponding numbers for concrete are 2 and 7 min, respectively, and 0.2 and 0.6 min for tunnels insulated with silicate boards. This means that the interaction of the wall temperatures to influence the mass burning rate of the fuel is not important in the early stages of the fire.

The flame volume above the fuel surface transfers radiation and convection $\dot{q}''_f$ to the burning surface. The flame volume and the gas temperature of the hot smoke above the fire becomes the dominating external source of radiation toward the fuel surface. The interactions with the fuel surface are governed by the 3D shape of the flame and gas volumes and its temperatures. The temperature in the zones above most open diffusion flames are often in the range of 800–900 °C rather than the 1200–1360 °C temperature range measured in tunnel fires. As radiation is absorbed by the flame volume and black smoke, the dominating radiation incident on the fuel surface is usually governed by conditions closer to the fuel surface. At the same time, $\dot{q}''_{rr}$ is the reradiation loss (note the minus sign) at the fuel surface. It can be written as $\dot{q}''_{rr} = \varepsilon\sigma T_s^4$ where L_g is the surface temperature of the fuel (here we assume ignition temperature) in Kelvin. In most cases, the view factor needs to be considered, but sometimes a value of one can be assumed in order to make a rough estimate.

In Eq. (4.2), $\Delta H_{c,eff}$ is the heat of combustion (kJ/kg) and L_g is the heat of gasification of the burning material (kJ/kg).

The $\dot{q}''_f$ varies from 22–77 kW/m^2 for large-scale flame heat fluxes [57]. For example assuming an 800 °C gas temperature corresponds to 75 kW/m^2, which correlate well the higher value of 77 kW/m^2. Babrauskas [58] show that for wood the heat flux can vary considerably depending on the exposure time. A value of $\dot{q}''_f = 25$ kW/m^2 seems reasonable for wood. Here it assumed that the flame volume behaves as an open fire, that is, the flame volume is in the vertical direction and does not deflect horizontally.

Example 4.2 What is $\dot{q}''$ for wood pallets assuming that $\dot{q}''_f = 25$ kW/m^2, $T_g = 100$ °C and $T_w = 10$ °C? Assume that F and ε are equal to one.

Solution: The following tabulated data [57] can be assumed for wood: $L_g = 1.8 \times 10^{3\,kJ/kg}$ *and* $\Delta H_{c,eff} = 13 \times 10^{3\,kJ/kg}$. *In the case when the pallets are burning with* $T_s = T_{ign}$ *(an ignition temperature of 300 °C for wood is a reasonable lower value for piloted ignition [58]),* $\dot{q}''_{rr} = 5.67 \times 10^{-11} \times (300 + 273)^4 = 6$ *kW/m*^{2}, $\dot{q}''_g = 5.67 \times 10^{-11} \times (100 + 273)^4 = 1.1$ *kW/m*^{2}, *and* $\dot{q}''_w = 5.67 \times 10^{-11} \times (10 + 273)^4 = 0.4$ *kW/m*^{2}. *The HRR*

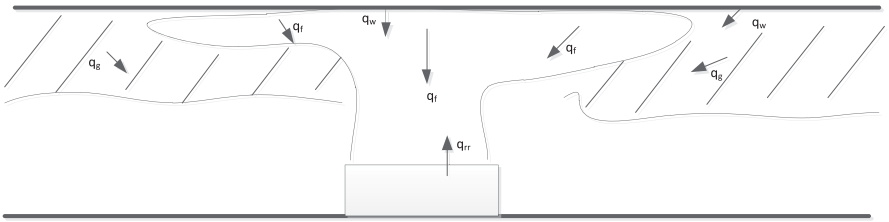

Fig. 4.11 Illustration of a large tunnel fire in which the flame deflects horizontally at the ceiling

per unit fuel surface area will be $\dot{q}'' = (25 + 1.1 + 0.4 - 6) \times 13/1.8 = 148$ *kW/m*^{2} *in accordance to Eq. (4.2). Tewarson [57] reported that* $\dot{q}''_{rr}$ *is equal to 10 kW/m*^{2} *for Douglas fir (wood). Using Tewarson's* $\dot{q}''_{rr}$ *value would lower the* $\dot{q}''$ *to 119 kW/m*^{2}.

This example shows that the increase in $\dot{q}''$ due to the gas or wall temperature is marginal in relation to many other parameters, especially the flame radiation $\dot{q}''_f$ and the ratio of $\Delta H_{c,\,eff}/L_g$ for fires in the early stages.

For a large fire scenario the flame volume will deflect at the ceiling and enhance the radiation from the deflected flame volume toward the fuel surface, see Fig. 4.11. The gas temperature will also be much higher. As mentioned earlier, the hot smoke and gases also radiate to the fuel surface. Simultaneously, the interaction of radiation is hampered by absorption and scattering in the flame volume and the hot smoke between the surfaces. The total heat balance and exchange are difficult to determine exactly, but Eq. (4.2) shows the most important parameters that are active in the process. The $\dot{q}''$ will most likely increase but at the same time there will be an attenuation of the radiation from the smoke (excluding the ceiling flame volume) and the tunnel walls. It is not certain that the $\dot{q}''$ will increase substantially even if the fire size increases as more fuel becomes involved and the large vertical flame volume and smoke could significantly hinder the radiation from the ceiling flame.

Although Eq. (4.2) is a simple relation, it shows the influence of the ceiling smoke layer and tunnel walls on the burning rate of the fuels burning inside a tunnel. This influence is perhaps not as large as one would expect, at least not during the important fire growth period that usually occurs within 10–20 min. There are other governing parameters, such as material properties, ventilation type and conditions, fuel geometry and tunnel height (deflection of flames) that are important. Also, one should bear in mind that this example assumes a line of sight between the fuel surface and the smoke layer surrounded by the tunnel surfaces, but in reality most fuels are geometrically complex. Most of the burning fuel surfaces do not have line of sight with the smoke layer and tunnel structure, but are hidden inside the fuel bed, or in vehicles. Also, note that the characteristic gas temperature further away is lower. The values of $\dot{q}''$ using Eq. (4.2) in the above analysis are probably conservative. In summary, the dominating parameter is the flame radiation and where radiation from gases and walls plays a less important role initially, but will contribute later in the fire development, although not nearly as much as the flame radiation. More information about the calculation of heat flux can be found in Chap. 10.

4.3.2 Effects of Tunnel Geometry

The effect of tunnel geometry on the HRR is an interesting research field. Carvel et al. [59] compared the increase of HRR due to tunnel geometry to similar situations in ambient outdoor conditions. A number of different experimental test series published in the literature were studied. The work included experiments involving liquid pools, wood cribs, and cars. The authors came to the conclusion that the width of the tunnel has a significant influence on the HRR from a fire in a tunnel. The results were explained by the surrounding wall and hot gas radiation to the pool surface, the temperature inside the tunnel, and the flow pattern near the fire. The analysis indicated that the height of the tunnel did not significantly affect the HRR enhancement.

Lönnermark and Ingason [60, 61] investigated the effect of geometry on the HRR using model scale tests and found that the dependency of the mass loss rate (MLR) and the HRR on the tunnel dimensions differ, especially for pool fires. Tests in a model-scale tunnel (scale 1:20) were performed to study the effect of the height and width of a tunnel on the MLR and the HRR. The tunnel was 10 m long. The widths used were 0.3, 0.45, and 0.6 m and the height was varied between 0.25 and 0.4 m. Two different types of fuels were used: pools of heptane and wood cribs. From the results it is clear that the dependency of the MLR and the HRR on the tunnel dimensions are different from each other, especially for pool fires. The results also indicate that the influence of tunnel dimensions is not only a radiation effect, as often assumed, but is probably a combination of radiation from surfaces and hot gases, influence of air flow patterns, the shape and position of the flame and combustion zone, and temperature distribution. The analysis shows that as several factors and processes are interacting, it is important to know the starting conditions to be able to predict the effect of a change in a specific parameter. In these tests the tunnel height was found to be the most important parameter influencing the enhanced HRR.

4.3.3 Effects of Ventilation on Peak HRR

The effect of longitudinal ventilation on the fire development of HGV fires has been of great interest among researchers and engineers for a long time. The use of critical velocity in the design of ventilation systems is one of the main reasons. When blowing high velocity air onto a fire, one should ask what the consequences on the HRR are. The interaction between the ventilation flow and the HRR has been thoroughly investigated by Carvel et al. [62–64]. In this chapter we will focus on the effects of ventilation on the peak HRR. In Chap. 5, the focus will be on fire growth.

The work carried out by Carvel's team at the Herriot–Watt University in Edinburgh was probabilistic in nature. The basis was that a Bayesian probabilistic approach was used to refine estimates made by a panel of experts and was combined with data from experimental fire tests in tunnels. The drawback of their work was

that their conclusions were based on rather limited experimental data and not on any physical experimental justifications. Fortunately, there has been new and more systematic research conducted in later studies with more consistent data [65–68].

In Carvel's studies it is stated that the size of HGV fires will be greatly increased by forced longitudinal ventilation. At a ventilation flow of 3 m/s such a fire will probably be four or five times larger than if natural ventilation was used. At 10 m/s the fire will probably be ten times larger. In their studies they used both wood crib tests, ordinary solid fuels, and vehicles. Neither the test results presented here nor estimates of HRR increases in vehicle fires show such a high increase as indicated by Carvel et al. The data on HRR per unit fuel surface area for vehicles presented earlier in this chapter cannot support the claim of a factor 4 to 10 increase for HGVs. These HRR values cannot physically be much larger than those obtained by Ingason and Li [66]. That is, the increase in peak HRR from ambient conditions is on the order of 1.4–1.55 for the ventilation rates tested (1.6–4.3 m/s in large scale) or by Lönnermark and Ingason [65] who showed that the increase in the peak HRR was in the range of 1.3–1.7 times the value measured outside the tunnel under ambient conditions. The only possible explanation for why Carvel et al. exhibited such a high increase in the peak HRR is due to the way the fuel was compared. Fuel that was ventilation controlled during ambient or natural ventilated conditions has probably been used in the comparison. If a fuel has a low porosity factor P, see definition in Sect. 4.3.4, the increase as presented by Carvel et al. can be easily obtained, which has been shown in Harmathy's work[69]. Harmathy had concluded that the heat released by the oxidation of the char plays an important role in the process of pyrolysis and thereby affects the HRR. Noncharring fuels (synthetic polymers) do not exhibit this influence on the HRR. This explains the increase in HRR due to ventilation obtained by Ingason and Li [66] who used charring material (wood cribs) in their model scale tests. This is crucial for our understanding of the effects of the ventilation rate on HRRs in tunnel fires.

The effects of ventilation on pool fires vary in the literature. Some show very little change in the mass burning rate and others show large effects. The trend in the experiments found in the literature is that these effects are larger for smaller pool fires as they are dominated by convective heat transfer from the flame volume, whereas larger pools are dominated by radiation heat flux from the flames. Therefore, the larger pool fires are less affected by the velocity.

Carvel et al. reported that the enhancing effect of ventilation for small pool fires is much less significant than that for HGV fires, while it increased by 50 % for large pool fires.

Ingason [70, 71] performed pool fire tests in a model-scale tunnel, using heptane, methanol, and xylene as fuels. For heptane, the maximum increase of the burning rate due to the tunnel was by a factor of 3.3 (0.13 kg/(m^2 s)) (u = 1 m/s) compared to 0.04 kg/(m^2 s) (free burn). Saito et al. [72] showed that the MLR for liquid fires increased in a tunnel compared to free burning conditions. The tests were performed with pool fires of methanol (0.1, 0.15, 0.2, and 0.25 m in diameter) and heptane (0.15 m in diameter). For the two smallest pools the effect of the tunnel (with an air velocity 0.08 m/s) on the MLR of methanol was only a few percent, while for the 0.25 m diameter pool the MLR in the tunnel was increased by a factor of 2.7

compared to freeburning conditions. For heptane, the tunnel (with an air velocity of 0.43 m/s) increased the MLR by approximately a factor of 4. For both fuels, the MLR was significantly decreased with increasing air velocity. This illustrates the importance of not only the ventilation and the tunnel cross-section but also the effects of the heat feedback from the flames, hot gases, and tunnel structure on the MLR.

Lönnermark and Ingason [61] performed a test series in a model-scale tunnel (1:20) and studied the effect of the width and the height of a tunnel on the MLR and HRR. They showed that the dependence of the MLR and the HRR on the tunnel dimensions are different from each other and that the effect of the height and the width of the tunnel on the MLR and HRR depends on the starting conditions. Here ventilation is an important factor.

Takeda and Akita studied the effects of tunnel conditions on fires and have also showed that the MLR and HRR are related to the ventilation factor [73]. They showed that the enhancement of the burning rate was associated with the dynamic balance between the rate of air supply and fuel gas supply.

Since, HGVs play such an important role for the outcome of fires in road tunnels [74], understanding the effect of the tunnel itself and of the air velocity inside the tunnel is important. One of the main problems when studying the effect of ventilation using different test series is that the conditions (tunnel dimension, starting ventilation conditions, etc.) vary between the test series. It is important to realise that several parameters affect the shape of the heat release curve, for example, the type of fuel used to represent the scenario, the air velocity inside the tunnel, and the tunnel geometry.

4.3.4 Fuel-Controlled Fires

According to Croce and Xin's experimental study of wood crib fires [75], the porosity of a wood crib is very important to determine if the wood crib is fuel controlled (well-ventilated) or ventilation controlled (under-ventilated). The porosity of a wood crib, P, is defined as:

$$P = \frac{A_v}{A_s} s^{1/2} b^{1/2} \tag{4.3}$$

where A_v is the total cross-sectional area of vertical crib shafts (m^2), A_s is the exposed surface area of the wood crib (m^2), s is the surface-to-surface spacing between adjacent sticks in a layer (m), and b is the stick thickness(with the same width and height) (m).

The porosity of a wood crib with the length L, the width l, and with a square cross-section of the sticks with the side b (see Fig. 4.12) can be defined as [60]:

$$P = \frac{A_v}{A_s} s_H^{1/2} b^{1/2} \tag{4.4}$$

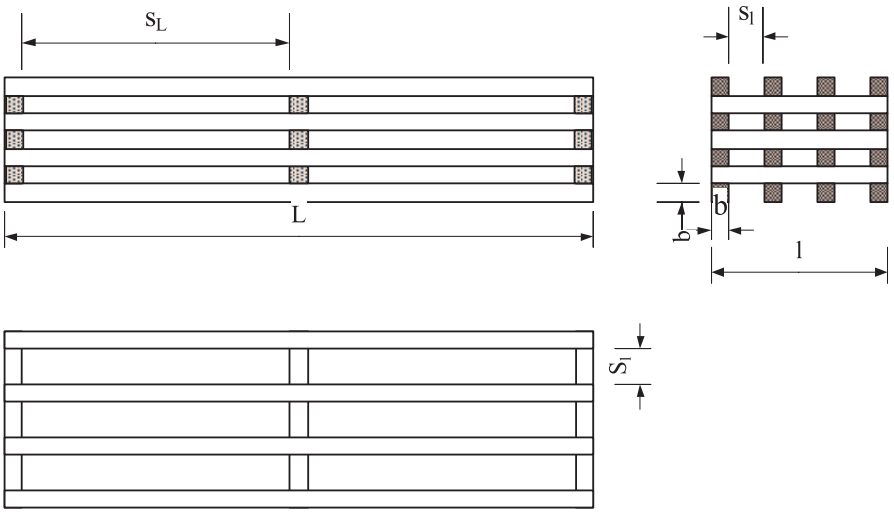

Fig. 4.12 Drawing of a wood crib and definition of different lengths [60]

where A_v is the total cross-sectional area of the vertical crib shafts

$$A_v = (L - n_l b)(l - n_L b) \tag{4.5}$$

and A_s is the total exposed surface area of the crib (based on the assumption that bottom and the top layers are with long sticks)

$$A_s = 4b(n_l N_l l + n_L N_L L) + 2b^2(n_l N_l + n_L N_L - n_l n_L N_L) - B \tag{4.6}$$

In the equation n_l, n_L, N_l, and N_L are the number of sticks in a layer with short sticks, the number of sticks in a layer with long sticks, the number of layers with short sticks, and the number of layers with long sticks, respectively. The parameter B is included to represent the area of the bottom of the wood crib that is not exposed. In the calculation of the porosity according to Eq. (4.4), the parameter s_H is included. This parameter corresponds to the hydraulic diameter of the rectangular space defined by the parameters $s_l = \left(\frac{l - n_L b}{n_L - 1}\right)$, $s_L = \left(\frac{L - n_l b}{n_l - 1}\right)$, and $s_H = \frac{2 s_l s_L}{s_l + s_L}$.

Equation (4.3) is used to calculate the porosity factor P (m) for square wood cribs used in research and Eq. (4.4) for long wood cribs in tunnel fire research.

The HRR increases rapidly with increasing porosity but this dependency weakens when the porosity is greater than 0.7 mm. In principal, this means that the HRR becomes a constant value as the cribs become more scattered.

For a solid fuel such as wood, the HRR is dependent on the net heat gained on the surfaces of the solid. This means that the total surface area is a very important parameter for combustion of solid fuels as the fire size becomes a multiplicand of the HRR per unit fuel surface area. Figure 4.13 shows the HRR per unit fuel surface

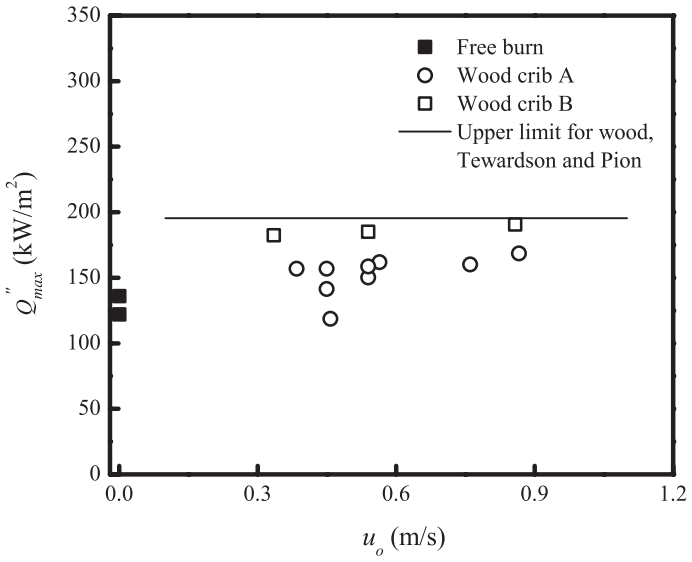

Fig. 4.13 The peak HRR per unit fuel surface area as a function of ventilation velocity [66]

area plotted against the ventilation velocity. It shows that the HRR per unit fuel surface area is a weak function of the ventilation velocity at best. The reason is that the fire is fuel-controlled[66]. An upper limit of the fuel MLR per unit fuel surface area presented by Tewarsonand Pion [76] for wood (Douglas fir) is 0.013 kg/(m^2 s), which correlates well with the experimental data given by Ingason and Li [66]. Based on data from model tunnel fire tests and from free burning tests(a test carried out without any boundary influences) they found that the fuel MLR per unit fuel surface area in a tunnel fire test is in a range of 1.4–1.55 times the value measured in a free burning test. If the value given by Tewarson and Pion is converted to HRR per fuel surface area of the wood cribs tested the $\dot{q}''$ corresponds to about 200 kW/m^2. This is shown as horizontal solid line in Fig. 4.13.

4.3.5 Ventilation-Controlled Fires

Ingason and Li [68] carried out model scale tests which could explain the region where a fire changes from fuel controlled to ventilation controlled. In the model scale tests conducted, the porosity P of the wood crib was chosen as 1.24 mm (>>0.7 mm)to minimize the effect of porosity on the HRR. This means that the wood crib should not show any type of ventilation control tendency during the tests.

The effect of the tunnel geometry and fire source was not investigated systematically in the study although data from two series of tests in model tunnels of different aspect ratios were used. The focus was on the analysis of the relationship between the HRR and ventilation velocity in the vicinity of the wood crib fuel.

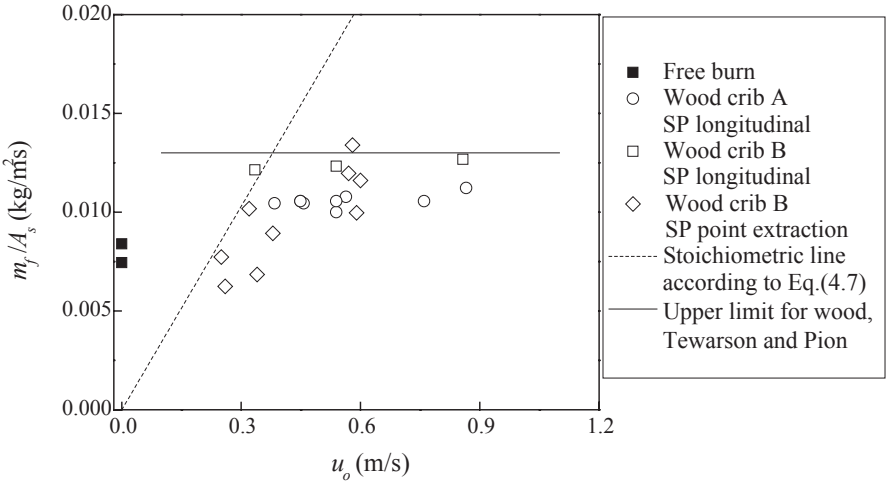

Fig. 4.14 The maximum fuel MLR per unit fuel surface area as a function of the ventilation velocity (single wood crib) [68]

Figure 4.14shows the fuel mass loss rate per unit area fuel surface against the ventilation velocity across the fire source. The stoichiometric fuel mass loss rate per unit fuel surface area is also given in Fig. 4.14. According to the principles of oxygen consumption, the stoichiometric fuel mass loss rate per fuel surface area, $\dot{m}_{f,stoi}$ (kg/(m^2 s)), can be expressed as:

$$\frac{\dot{m}_{f,stoi}}{A_s} = \frac{\dot{Q}}{\chi \Delta H_c A_s} = 0.24 \frac{A}{A_s} u_o \tag{4.7}$$

where A is the tunnel cross-sectional area (m^2), A_s is the fuel surface area(m^2) and u_o is the tunnel longitudinal velocity (m/s).

It is shown in Fig. 4.14 that for a longitudinal ventilation velocity less than 0.35 m/s the fuel MLR per unit fuel surface area increases with the ventilation velocity and follows the stoichiometric line. This indicates that the fire under these conditions is ventilation controlled. However, when the ventilation velocity rises above 0.35 m/s (1.6 m/s in large-scale) the fire is no longer sensitive to the ventilation velocity. This indicates that the fire becomes fuel-controlled. The upper limit of the fuel MLR per unit fuel surface area was about 0.013 kg/(m^2 s).It is also shown in Fig. 4.14 that within a range of 0.35–0.9 m/s, the fuel MLR per unit fuel surface area tends to be a weak function of velocity. However, it can be expected that the fuel MLR per unit fuel surface area will begin to decrease when the ventilation velocity is greater than a certain value due to the cooling effect of the ventilation. Comparing the data in tunnel fire tests and that in a free burning test shows that the ratio of fuel MLR per unit fuel surface area in a tunnel fire to that in a free burning test is about 1.5 in the constant region (fuel controlled), and that it can be less than 1 if the tunnel is ventilation controlled or influenced by vitiation as described in Chap. 2.

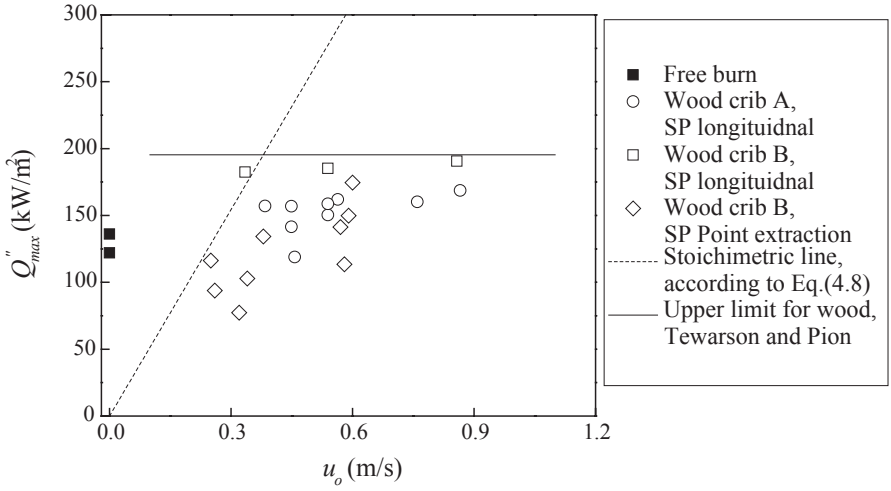

Fig. 4.15 The peak HRR per unit fuel surface area vs. ventilation velocity [68]

The above analysis is based on the fuel MLR of a single wood crib. In some tests, several wood cribs were burnt together and the total HRR was measured using the oxygen calorimetry technique rather than measuring the MLR.

Figure 4.15 shows the peak HRR per unit fuel surface area as a function of the ventilation velocity. The stoichiometric HRR per fuel surface area is plotted as a sloped solid line. For a fire with several wood cribs, the total fuel surface area was used. According to the principles of oxygen consumption, the stoichiometric HRR per fuel surface area, $\dot{Q}''_{stoi}$ (kW/m^2), can be expressed as:

$$\dot{Q}''_{stoi} = \frac{\dot{Q}}{A_s} = 3600 \frac{A}{A_s} u_o \tag{4.8}$$

The same trend is shown in Fig. 4.15 as in Fig. 4.14, although the data does not correlate as well. The reason is that in a test with several wood cribs, all surfaces of these wood cribs did not burn simultaneously. When the peak HRR occurred, part of the first wood crib had already started to decay. As a consequence, the peak HRR divided by the total fuel surface area is slightly lower for the case with several wood cribs compared to a single crib.

4.4 HRR per Exposed Fuel Surface Area

Ingason [6] has emphasized the importance of using and reporting HRR data given as MW/m^2 or kW/m^2 exposed fuel surface, or $\dot{q}''$. The main reason is the enormous variation in HRR data for each type of vehicle that uses transport tunnels or other underground spaces. By estimating the exposed fuel area of a vehicle it is possible

Table 4.7 The HRR parameters for different materials in Eq. (4.2) [57]

Type of material	$\dot{q}''_{rr}$ (kW/m^2)	L_g (kJ/g)	$\Delta H_{c,eff}$ (kJ/g)	$\dot{q}''_f$ (kW/m^2)	$\dot{q}''$ (kW/m^2)	HRP
Hexane	0.63	0.55	42.2	37	2791	77
Heptane	0.98	0.6	41	37	2461	68
Kerosene	1	0.85	40.3	29	1316	47
Polyethylene	15	2	38.4	61	883	19
Polystyrene	11.5	1.6	27	75	1072	17
Polyurethane (flexible)	17.5	1.95	17.8	70	479	9
Polyurethane (rigid)	18	3.25	16.4	51	167	5
PVC	10	1.7	5.7	50	134	3
Corrugated paper	10	2.2	13.2	25	90	6
Wood	10	1.8	13	25	108	7

to get a very good estimate of the peak HRR. Exposed fuel surface is defined here as the area where combustion/pyrolysis can possibly occur, that is, a fuel surface that is exposed to high incident heat radiation with enough oxygen to maintain combustion. For a box, the exposed fuel surface area is the sum of the outer surfaces, and not what is inside the box, whereas a seat can burn on all sides. A pile of wood pallets can burn on the surfaces that are exposed to air but when the pile falls down, the exposed surface area may increase rapidly and the peak HRR increases correspondingly.

Information can also be obtained by doing fire tests of only small portions of the cargo or the vehicle. This was done prior to the Runehamar tests in 2003 where, based on information from preliminary laboratory tests, the peak HRRs could be predicted with acceptable accuracy for three of the test commodities [11]. A summary of this data is given in references [6] and [9].

The ratio $\Delta H_{c,\,eff}/L_g$ has been given the name "Heat Release Parameter" (HRP) by Tewarson [57]. In order to explore the importance of the different parameters in Eq. (4.2) we can look at the range of values given by Tewarson[57], see Table 4.7.

Table 4.7 clearly shows the importance of the HRP to predict values of $\dot{q}''$ for different materials. The other parameters are also important, especially the total flame heat flux $\dot{q}''_f$ and the reradiation $\dot{q}''_{rr}$ which is related to the ignition temperature.

The values presented in Table 4.7 appear to have some correlation to the values presented by Ingason [6]. As is shown in Table 4.8 in Sect. 4.4.2, for different solid materials, $\dot{q}''$ ranges from 70 kW/m^2 for wood cribs to 500 kW/m^2 for furniture having a mixture of polyurethane foam, wood and plastics. For liquid fires the $\dot{q}''$ are in the same range as found in Table 4.7, see Sect. 4.4.1. The values of calculated HRR per fuel surface area for wood provided by Tewarson correspond well to those found in Table 4.8 for wood pallets, where $\dot{q}''$ was found to vary between 110 and 160 kW/m^2, see Sect. 4.4.2.

Table 4.8 Summary of HRR per fuel surface area for solid materials applied in large-scale tunnel fire tests [6, 9]

Type of fuel	Test series	Estimated fuel surface area (m^2)	HRR per square metre fuel surface area at maximum (MW/m^2)
Wood cribs	EUREKA (test 8, 9, and 10)	140	0.07–0.09
Wood pallets	2nd Benelux (tests 8, 9, 10, and 14)	120 (36 pallets) 240 (72 pallets)	0.11–0.16
82 % wood pallets and 18 % PE pallets	Runehamar (test 1)	1200	0.17
82 % wood pallets and 18 % PUR matrasses	Runehamar (test 2)	630	0.25
81 % wood pallets and cartons and 19 % plastic cups	Runehamar (test 4)	160	0.44
HGV-furniture	Runehamar (test 3)	240	0.5
HGV-furniture	EUREKA (test 21)	300	0.4
Runehamar 2013	Runehamar 2013	1470	0.06
Singapore 2012 80 % wood pallets and 20 % PE pallets	Singapore 2012	910	0.17
Rubber tyres	Diverse		0.11–0.21

4.4.1 Liquids

In Table 4.5, a summary of HRRs of all liquid pool fire tests and other relevant tests was shown, comparisons to Eq. (4.1) were also included. The comparison shows a good correspondence wherever the effects of ventilation were not dominant.

In Table 4.7, $\dot{q}''$ values for heptane and kerosene are presented. The values are 2.46 MW/m^2 for heptane and 1.32 MW/m^2 for kerosene, respectively. These values correspond well to fires reported or calculated using Eq. (4.2) having an area of about 0.4 m^2.

The variation in test results is considerable and it is difficult to assume one value for each type of liquid fuel. Parameters that influence the burning rate for each fuel type are the fuel pan geometry, the fuel depth, the ventilation conditions, and the tunnel geometry. In cases where the tunnel cross-section is large and the width of the pan is much smaller than the width of the tunnel, the influence of longitudinal ventilation on the burning rate appears to be small. If the fuel bed has about the same width as the tunnel the fire size is reduced. These effects increase as the length of the pan increases.

4.4.2 Solid Materials

In many of the large-scale tests presented in Chap. 3, solid materials such as pallets, cartons, or wood cribs have been used. It is of interest to compare the peak HRR per unit fuel surface area in order to see if these values are comparable between the tests series. This type of information could be used when estimating the peak HRR from HGV trailers with a tarpaulin as cargo coverage. In Table 4.8 a summary of the HRR per unit fuel surface area is given for tests that included solid materials based on the data presented in this chapter and in Chap. 3.

Tests that included solid wood cribs or pallets are found in the TUB-VTT tests, the EUREKA test series, and the 2nd Benelux tests. In the Runehamar tests wood pallets (about 82 % of the total mass) were integrated with other types of solid materials such as plastics (18 % of the total mass), cartons and,furniture and fixtures.

In the 2nd Benelux tests with wood pallets the HRR per unit fuel surface area varied between 0.11–0.16 MW/m^2 with an average value of 0.13 MW/m^2.This value tended to increase with increased ventilation rate. The fuel itself was not densely packed and thus could be regarded as fuel surface controlled. For wood cribs the opposite fire condition would be crib porosity controlled or ventilation controlled. In the EUREKA tests using a simulated truck load the wood sticks were so densely packed that the fire became crib porosity controlled (ventilation controlled) under normal conditions. This means that the peak HRR became lower than if it was fuel surface controlled. In the simulated truck load fire test, the HRR per unit fuel surface area was estimated to be in the order 0.04 MW/m^2. In the wood crib tests in the EUREKA test series the HRR varied between 0.07–0.09 MW/m^2 depending on the longitudinal velocity. It was not possible to establish with any certainty whether the wood cribs were fuel surface or crib porosity controlled. In the Runehamar tests in 2013, 441 pallets were used with a peak HRR of 79 MW in one of the tests, which was a free burn test, that is, no water spray was used. The fuel surface area of the pallets was estimated to be 3.3 m^2 and the peak HRR per unit fuel surface area was 0.06 MW/m^2, which is slightly less than the results from other tests. In the Singapore tests in 2012, 80 % of the fuel was wood pallets and 20 % was polyethylene pallets. The HRR per unit fuel surface was then 0.17 MW/m^2, assuming the surface area of the pallets to be 3.3 m^2. This is exactly the same value as obtained in the Runehamar test number 1 in 2003.

In the HGV test in the EUREKA 499 test series using furniture the HRR per unit fuel surface area was estimated to be approximately 0.4 MW/m^2. The total fuel surface of the furniture commodity was estimated to be about 300 m^2 and the peak HRR was120 MW.

The HRR per unit fuel surface area in the Runehamar tests was estimated to be about 0.17 MW/m^2 for test 1 with wood and plastic pallets, 0.25 MW/m^2 for test 2 with wood pallets and mattresses, 0.5 MW/m^2 for test 3 with furniture and fixtures and 0.44 MW/m^2 for test 4 with plastic cups in cartons.

In the large-scale tests presented here, the peak HRR for solid materials ranges from 0.07 to about 0.5 MW/m^2. An interesting observation is that the furniture tests

in the EUREKA 499 and Runehamar test series appear to be in the same order of magnitude. The reason is that both tests were performed under good ventilation conditions and that the fuel surface area was similar. The fuel surface area was estimated to be roughly 300 m^2 in the EUREKA 499 test and about 240 m^2 in the Runehamar test 2003. With this type of information it would be easy to estimate the peak HRR for a given type of fuel in a HGV fire.

For rubber tyres it is possible to estimate the HRR based on information given earlier in this chapter. Rough estimation indicates that the peak HRR for rubber tyres per exposed surface area is in the range of 0.11–0.21 MW/m^2. This information can be used to estimate the peak HRR for a certain size of a rubber tyre. One should also keep in mind that there is an important difference between the SINTEF test and the other tests, namely the presence of the rim in the SINTEF tests and the way the passenger car tyres were piled up, which may influence the estimation of the exposed fuel surface area. If the SINTEF tests are removed then the range of HRRs for rubber tyres per exposed external area is 0.11–0.15 MW/m^2.

Ingason and Hammarström [50] estimated the area when the tyre reached the first clear peak HRR to be 5.9 m^2. They argued that if they subtract the contribution from the diesel fire which was about 1.1 MW, they would have approximately 1.3 MW from the tyre. This means that the HRR per unit fuel surface area at this time was 0.20 MW/m^2. This is in line with the results obtained from other studies mentioned earlier. In this test, after the first HRR peak, the fire intensity decreased and the next abrupt increase occurred after about 70 min, when both sides of the tyre were fully involved in the fire and gases were coming from the inside of the tyre. The total exposed exterior fuel surface area of the tyre was about 8 m^2, meaning that the HRR per unit fuel surface area was about 0.25 MW/m^2.

4.4.3 Vehicle Fires

Vehicle fires can be either fuel controlled or ventilation controlled, depending on the fuels and openings available. According to Li et al's work [77], for a ventilation controlled vehicle fire, the openings available, including both the initial openings and those created during the fire, dictate the level of the peak HRR. The peak HRR in these tests can be estimated based on full consumption of the oxygen flowing in through the openings multiplied by a correction factor, which depends on the heat absorbed by the fuel surfaces and the fuels available. The heat absorbed by the surfaces is directly proportional to the heat of combustion and inversely proportional to the heat of pyrolysis. In addition, the fraction of the fuel surfaces exposed to the fire also has a strong influence on the peak HRR. In contrast, for a fuel-controlled vehicle fire, the peak HRR can be simply estimated by superposition.

In the following text a summary of the peak HRRs for different types of vehicles is given for the large-scale tests presented here. The data is presented in Table 4.8 as HRR per unit fuel surface area. It is only possible to present the cases where the fire was probably not ventilation controlled at peak conditions. In many of the vehicle

fires the enclosure structure of the vehicle (body) was burned off (For example, bodies made of aluminium, plastic, composite materials, etc.) allowing oxygen to become entrained in the fire plume. In some cases the enclosure was kept intact but the windows were large enough to preserve a fuel-controlled fire. However, in some of the tests the opening area of the windows controlled the HRR. In tests 12 and 13 with train wagons in the EUREKA 499 test series the fire developed very slowly due to the windows. The fire became ventilation-controlled and spread along the train wagon (steel body) at the same speed as the windows cracked due to the heat. In these tests the information on the fuel surface area is impossible to estimate, therefore, they have been excluded from the table.

Fully developed fires in passenger cars with steel bodies can be regarded as fuel surface controlled fires due to the large window area in comparison with the fuel surface area and the window height. This is not a generic condition as many modern cars have windows that do not necessarily break when a fire starts inside the car. The ventilation factor [78] for medium sized passenger cars is estimated to be in the range of 1.2–1.8, which is considerably higher than the limits for fuel-controlled enclosure fires (0.29) with wood cribs [78]. The peak HRR for single passenger cars (small and large) vary from 1.5–8 MW, but the majority of the tests show peak HRR values less than 5 MW [5]. When two cars are involved in the fire the peak HRR varies between 3.5 and 10 MW. The time to reach peak HRR varies between 10 and 55 min. The fuel surface area of the interior of a medium sized passenger car can be estimated to be in the range of 12–18 m^2. This includes the floor and ceiling area, instrument panel area, door area and the seat area (double sided).This would mean that the HRR per unit fuel surface area of a passenger car with a peak HRR of 5 MW can vary between 0.3–0.4 MW/m^2. The only test in a tunnel available is test no 20 in the EUREKA 499 test program. The car was a Renault Espace J11 with a plastic body. This car developed a peak HRR of 6 MW and the fuel surface area was estimated to be about 17 m^2, not including the ceiling.

Other vehicles with fuel-controlled fires were the tests 7, 11, 14, and 20 in the EUREKA 499 program, see Chap. 3, Sect. 3.3.7. In these tests, the main contribution is from the floor material and the seats. In tests carried out for different clients at SP Fire Research in Borås Sweden it was seen that fires in seats reach a peak HRR per unit fuel surface area of between 0.2 and 0.5 MW/m^2. This includes both bus seats and train seats. In Table 4.9, one can see that the total HRR per unit fuel surface area is in line with these values. It ranges between 0.20–0.38 MW/m^2. In a train there are numerous different materials in the interior of a coach or wagon. This material can be anything from textile, rubber, foam padding, PVC, cork, etc. What is interesting here is that the HRR per unit fuel surface area in fuel-controlled fires in different vehicles falls into a rather narrow range between 0.2 and 0.4 MW/m^2. This is also in line with the HRR per unit fuel surface area for the solid materials presented in Table 4.7. The HRR per unit fuel surface area of the individual materials have a greater variation, both lower and much higher, but it appears that the total effect of the mixed materials is not that broad.

Table 4.9 The summary of HRR per unit fuel surface area of vehicles with fuel-controlled fires [6, 9]

Type of fuel	Test series	Estimated fuel surface area (m^2)	HRR per square metre at maximum MW/m^2
Medium sized passenger cars	Assuming a 5 MW fire in the car	12–18	0.3–0.4
Passenger car plastic	Test 20 in EUREKA	17 (no ceiling)	0.35
Buss	Test 7 in EUREKA	80	0.36
Train	Test 11 in EUREKA	145	0.30
Subway coach	Test 14 in EUREKA	130	0.27
METRO tests	Test 2 and 3	230	0.33
Carleton laboratory facility	Intercity train	150	0.2
Carleton laboratory facility	Subway coach	130	0.38

4.5 Summary

Ingason [6] collected HRR data from all the large-scale tests available in the literature and normalized the peak HRR to the exposed fuel surface area. The fuel surface area was defined as the freely exposed area where release of gasified or vaporized fuel can occur. The reason for normalizing test data to the exposed fuel surface area was that this makes it convenient to compare the peak HRRs between different types of fuels and for different fire conditions. The results may be used to help estimate the peak HRR in different types of vehicles and with other solid and liquid fuels. Based on this work, the HRR data were divided into three different groups according to fuel type: liquid pool fires, ordinary solid materials such as wood pallets and wood cribs, and road and rail/metro vehicles.

It is important to understand how the reported HRRs were measured or calculated in order to make valid comparisons. Multiple car fire tests are mainly conducted in low ceiling car parks with nearly no longitudinal ventilation. The ignition source and location is a major factor for the time to reach the peak HRR for buses, as well as the body material of the bus (glass fibre, steel, aluminium, etc.). The type of cargo containment (tarpaulin, aluminium, steel, etc.) is very important for HGV fires, as well as the combustible material and the ventilation conditions. The ignition source and location is also an important factor on the time to reach a peak HRR for HGV fires. Any type of interaction with a water based spray system must also be considered as it significantly interacts with the combustible material and the environment.

It was concluded, based on the experimental tests considered so far, that the peak HRR per unit fuel surface area in a fuel-controlled fire for different vehicles is approximately between 0.2 and 0.4 MW/m^2 [6]; although, when HGV trailer mock-ups are included, this becomes about 0.2–0.5 MW/m^2. This is also in line with the

HRR per unit fuel surface area for solid materials. The HRR per unit fuel surface area for each individual material exhibits a greater variation, but it appears that the total effect of the mixed material leads to a narrow range of HRR values. This observation is very important to consider when establishing design fires for tunnels. It is essential to realize, however, that this is an initial finding; it is based upon tests in which the ventilation velocities have ranged from about 0.5 to about 6 m/s. In a real-world situation the ventilation velocity may be higher than 6 m/s (For example, there may be a natural wind). As a general rule, the total HRR for a single vehicle or item/fuel package in a tunnel fire depends on many factors. Further, the total HRR depends upon the potentiality for spread from one item to another. That is, the proximity of items (For example, vehicles) is of crucial importance. Therefore, it is very important to perform more large-scale tunnel fire tests using real vehicles to test these initial observations. Most of the existing vehicle fire data are for outdated vehicles, and therefore, a new large-scale tunnel test series with modern road and rail/metro vehicles is a pressing scientific need.

The other parameter of interest is the time to reach a peak HRR value. The data in Table 4.1 show that there is a great variety in the time to reach peak HRR. This time varies between 10 and 55 min.

The large-scale tests show that in a real tanker fire accident, where it is realistic to expect that the gasoline spreads over the entire tunnel width, one can expect the HRR per unit fuel surface area to be in the range of 0.35–2.6 MW/m^2 depending on the ventilation conditions and spread of the fuel over the road surface. In well-ventilated conditions with pan fuel depth that is larger than 70 mm and where the pan width is smaller than the tunnel width the HRR is expected to be about 2.4–2.6 MW/m^2 for gasoline. The effects of the fuel depth on the burning rate have not been considered here but in a real accident the burning rate could be reduced due to the cooling effect of the road surface.

References

1. Fire and Smoke Control in Road Tunnels (1999), PIARC
2. NFPA 502 (2004) Standard for Road Tunnels, Bridges, and other Limited Access Highways. 2004 edn. National Fire Protection Association
3. Ingason H An Overview of Vehicle Fires in Tunnels. In: Vardy A (ed) Fourth International Conference on Safety in Road and Rail Tunnels, Madrid, Spain, 2–6 April, 2001. pp. 425–434
4. Lönnermark A, Ingason H (2005) Gas Temperatures in Heavy Goods Vehicle Fires in Tunnels. Fire Safety Journal 40:506–527
5. Ingason H, Lönnermark A Recent Achievements Regarding Measuring of Time-heat and Time-temperature Development in Tunnels. In: 1st International Symposium on Safe & Reliable Tunnels, Prague, Czech Republic, 4–6 February 2004. pp 87–96
6. Ingason H (2006) Fire Testing in Road and Railway Tunnels. In: Apted V (ed) Flammability testing of materials used in construction, transport and mining. Woodhead Publishing, pp 231–274

7. Babrauskas V (2008) Heat Release Rates. In: DiNenno PJ, Drysdale D, Beyler CL et al. (eds) The SFPE Handbook of Fire Protection Engineering. Fourth Edition edn. National Fire Protection Association, Quincy, MA, USA, pp 3–1–3–59
8. Beard AN, Carvel RO (2012) Handbook of tunnel fire safety—Second Edition. ICE Publishing
9. Ingason H, Lönnermark A (2012) Heat Release Rates in Tunnel Fires: A Summary. In: Beard A, Carvel R (eds) In The Handbook of Tunnel Fire Safety, 2nd edition. ICE Publishing, London
10. Ingason H Heat Release Rate Measurements in Tunnel Fires. In: Ivarson E (ed) International Conference on Fires in Tunnels, Borås, Sweden, October 10–11, 1994 1994. SP Swedish National Testing and Research Institute, pp 86–103
11. Ingason H, Lönnermark A Large-scale Fire Tests in the Runehamar tunn—Heat Release Rate (HRR). In: Ingason H (ed) International Symposium on Catastrophic Tunnel Fires (CTF), Borås, Sweden, 20–21 November 2003. SP Swedish National Testing and Research Institute, pp SP Report 2004:2005, p. 2081–2092
12. Steinert C Smoke and Heat Production in Tunnel Fires. In: The International Conference on Fires in Tunnels, Borås, Sweden, 10–11 October 1994. SP Swedish National Testing and Research Institute, pp 123–137
13. Axelsson J, Andersson P, Lönnermark A, van Hees P, Wetterlund I (2001) Uncertainties in Measuring Heat and Smoke Release Rates in the Room/Corner Test and the SBI. SP Swedish National Testing and Research Institute, Borås, Sweden
14. Ingason H, Gustavsson S, Dahlberg M (1994) Heat Release Rate Measurements in Tunnel Fires. SP Swedish National Testing and Research Institute, Borås, Sweden
15. Fires in Transport Tunnels: Report on Full-Scale Tests (1995). edited by Studiensgesellschaft Stahlanwendung e. V., Düsseldorf, Germany
16. Proceedings of the International Conference on Fires in Tunnels (SP Report 1994:54). SP Swedish National Testing and Research Institute Borås, Sweden
17. Ingason H, Lönnermark A (2005) Heat Release Rates from Heavy Goods Vehicle Trailers in Tunnels. Fire Safety Journal 40:646–668
18. Karlsson B, Quintier JG (2000) Enclosure Fire Dynamics. CRC Press,
19. Mangs J, Keski-Rahkonen O (1994) Characterization of the Fire Behavior of a Burning Passenger Car. Part II: Parametrization of Measured Rate of Heat Release Curves. Fire Safety Journal 23:37–49
20. Steinert C (2000) Experimentelle Untersuchhungen zum Abbrand-und Feuerubersprungsverhalten von Personenkraftwagen. vfdb-Zeitschrift, Forschung, Technik und Management im Brandschutz 4:163–172
21. Ingason H, Nireus K, Werling P (1997) Fire Tests in a Blasted Rock Tunnel. FOA, Sweden
22. Shipp M, Spearpoint M (1995) Measurements of the Severity of Fires Involving Private Motor Vehicles. Fire and Materials Vol. 19:143–151
23. Lemaire A, van de Leur PHE, Kenyon YM (2002) Safety Proef: TNO Metingen Beneluxtunnel—Meetrapport. TNO
24. Joyeux D (1997) Development of Design Rules for Steel Structures Subjected to Natural Fires in Closed Car Parks. Centre Technique Industriel de la Construction Métallique, Saint-Rémy-lès-Chevreuse, France
25. Shipp M, Fraser-Mitchell J, Chitty R, Cullinan R, Crowder D, Clark P (2009) Fire Spread in Car Parks. Fire Safety Engineering (June):14–18
26. Joyeux D (1997) Natural Fires in Closed Car Parks—Car Fire Tests, INC-96/294d-DJ/NB.
27. Lönnermark A (2005) On the Characteristics of Fires in Tunnels. Doctoral Thesis, Doctoral thesis, Department of Fire Safety Engineering, Lund University, Lund, Sweden
28. Axelsson J, Försth M, Hammarström R, Johansson P (2008) Bus Fire Safety. SP Technical Research Institute of Sweden, Borås, Sweden
29. Kunikane Y, Kawabata N, Ishikawa T, Takekuni K, Shimoda A Thermal Fumes and Smoke Induced by Bus Fire Accident in Large Cross Sectional Tunnel. In: The fifth JSME-KSME Fluids Engineering Conference, Nagoya, Japan, 17–21 November 2002.

30. Haack A Introduction to the Eureka-EU 499 Firetun Project. In: Proceedings of the International Conference on Fires in Tunnels, SP Report 1994:54, Borås, Sweden, 1994
31. Brousse B, Perard M, Voeltzel A, Botlan YL Ventilation and fire tests in the Mont Blanc Tunnel to better understand the catastrophic fire of March 24th, 1999. In: Third international conference on Tunnel Fires and Escape from tunnels, Washington DC, USA, 9–11 October 2001. pp 211–222
32. Brousse B, Voeltzel A, Botlan YL, Ruffin E (2002) Mont Blanc tunnel ventilation and fire tests. Tunnel Management International Vol. 5, Nr 1:13–22
33. MK C, WO C, KW L, AD L, LM N, F T Heat release rates of heavy goods vehicle fires in tunnels. In: In: 15th International Symposium on Aerodynamics, Ventilation & Fire in Tunnels, Barcelona, Spain, 2013. BHR Group, pp 779–788
34. Cheong MK, Cheong WO, Leong KW, Lemaire AD, LM N (2013) Heat Release Rates of Heavy Goods Vehicle Fire in Tunnels with Fire Suppression System. Fire Technology. doi:10.1007/s10694-013-0367-0
35. Ingason H, Appel G, Li YZ, Lundström U, Becker C Large scale fire tests with a Fixed Fire Fighting System (FFFS). In: ISTSS 6th International Symposium on Tunnel Safety and Security, Marseille, 2014
36. Grant GB, Drysdale D Estimating Heat Release Rates from Large-scale Tunnel Fires. In: Fire Safety Science—Proceedings of the Fifth International Symposium, Melbourne, 1995. pp 1213–1224
37. Chuang Y-J, Tang C-H, Chen P-H, Lin C-Y (2005–2006) Experimental investigation of burning scenario of loaded 3.49-ton pickup trucks. Journal of Applied Fire Science 14 (1):pp 27–46
38. A. Kashef, J. Viegas, A. Mos, N H Proposed idealized design fire curves for road tunnels. In: 14th International Symposium on Aerodynamics and Ventilation of Tunnels, Dundee, Scotland 11–13 May, 2011
39. Heselden A Studies of fire and smoke behavior relevant to tunnels. In: 2nd Int Symp on Aerodynamics and Ventilation of Vehicle Tunnels, Cambridge, UK, 23–25 March 1976. Paper J1, BHRA Fluid Engineering, pp J1–1–J1–18
40. Liew S, Deaves D Safety Assessment of Dangerous Goods Transport in a Road Tunnel. In: Safety in Road and Rail Tunnels, First International Conference, Basel, Switzerland, 23rd–25th November 1992. pp 227–237
41. Larson DW, Reese RT, Wilmot EL The Caldecott Tunnel Fire Thermal Environments, Regulatory Considerations and Probabilities. Sandia National Laboratories
42. Caldecott Tunnel Near Oakland California, April 7, 1982 (Highway Accident Report Report No. 3665A.). Highway Accident Report Report No. 3665A. National Transportation Safety Board Washington D. C
43. Ingason H Small Scale Test of a Road Tanker Fire. In: Ivarson E (ed) International Conference on Fires in Tunnels, Borås, Sweden, October 10–11 1994. SP Swedish National Testing and Research Institute, pp. 238–248
44. Babrauskas V (2002) Heat Release Rates. In: DiNenno PJ, Drysdale D, Beyler CL et al. (eds) The SFPE Handbook of Fire Protection Engineering. Third edition edn. National Fire Protection Association, Quincy, MA, USA, pp 3–1–3–37
45. Zabetakis MG, Burgess DS (1961) Research on the hazards associated with the production and handling of liquid hydrogen. US Bureau of Mines, Pittsburgh, PA
46. Schlussbericht der Versuche im Ofenegg Tunnel von 17.5–31.5 1965 (1965). Kommission für Sicherheitsmassnahmen in Strassentunneln
47. ILF (1976) Brandversuche in einem Tunnel. Ingenieurgemeinschaft Lässer-Feizlmayr; Bundesministerium f. Bauten u. Technik, Strassenforschung
48. Lönnermark A, Kristensson P, Helltegen M, Bobert M Fire suppression and structure protection for cargo train tunnels: Macadam and HotFoam. In: Lönnermark A, Ingason H (eds) 3rd International Symposium on Safety and Security in Tunnels (ISTSS 2008), Stockholm, Sweden, 12–14 March 2008. SP Technical Research Institute of Sweden, pp 217–228

49. Hansen R, Ingason H (2013) Heat release rate measurements of burning mining vehicles in an underground mine. Fire Safety Journal 61 12–25
50. Ingason H, Hammarström R (2010) Fire test with a front wheel loader rubber tire. SP Technical Research Institute of Sweden, SP Report 2010:64
51. Shipp MP, Guy PS (1993) Fire Behaviour of Rubber Tyres. Fire Research Station report TCR 65/93
52. Hansen PA (1995) Fires in Tyres—Heat Release Rate and Response of Vehicles. SINTEF—Norwegian Fire Research Laboratory
53. Lönnermark A, Blomqvist P (2005) Emissions from Tyre Fires. SP Swedish National Testing and Research Institute, Borås, Sweden
54. Lönnermark A, Lindström J, Li YZ, Claesson A, Kumm M, Ingason H (2012) Full-scale fire tests with a commuter train in a tunnel. SP Technical Research Institute of Sweden, Borås, Sweden
55. Hadjisophocleous G, Lee DH, Park WH Full-scale Experiments for Heat Release Rate Measurements of Railcar Fires. In: International Symposium on Tunnel Safety and Security (ISTSS), New York, 2012. SP Technical Research Institute of Sweden, pp 457–466
56. Barber C, Gardiner A, Law M Structural Fire Design of the Øresund Tunnel. In: Ivarson E (ed) Proceedings of the International Conference on Fires in Tunnels, Borås, Sweden, 10–11 October 1994. SP Swedish National Testing and Research Institute, pp 313–332
57. Tewarson A (2002) Generation of Heat and Chemical Compounds in Fires. In: DiNenno PJ, Drysdale D, Beyler CL et al. (eds) The 3rd edition of SFPE Handbook of Fire Protection Engineering. Third edition edn. National Fire Protection Association, Quincy, MA, USA, pp 3–82–83–161
58. Babrauskas V Ignition of Wood—A Review of the State of the Art. In: Interflam 2001, Edinburgh, Scotland, 17–19 September 2001. Interscience Communications Ltd., pp 71–88
59. Carvel RO, Beard AN, Jowitt PW How Much do Tunnels Enhance the Heat Release Rate of Fires? In: Proc. 4th Int. Conf on Safety in Road and Rail Tunnels, Madrid, Spain, 2–6 April 2001. pp 457–466
60. Lönnermark A, Ingason H (2007) The Effect of Cross-sectional Area and Air Velocity on the Conditions in a Tunnel during a Fire. SP Report 2007:05. SP Technical Research Institute of Sweden, Borås, Sweden
61. Lönnermark A, Ingason H The Influence of Tunnel Dimensions on Fire Size. In: Proceedings of the 11th International Fire Science & Engineering Conference (Interflam 2007), London, UK, 3–5 September 2007. Interscience Communications, pp 1327–1338
62. Carvel RO, Beard AN, Jowitt PW, Drysdale DD (2001) Variation of Heat Release Rate with Forced Longitudinal Ventilation for Vehicle Fires in Tunnels. Fire Safety Journal 36 (6):569–596
63. Carvel RO, Beard AN, Jowitt PW (2001) The Influence of Longitudinal Ventilation Systems on Fires in Tunnels. Tunnelling and Underground Space Technology 16:3–21
64. Carvel RO, Beard AN, Jowitt PW The Influence of Longitudinal Ventilation and Tunnel Size on HGV Fires in Tunnel. In: 10th International Fire Science & Engineering Conference (Interflam 2004), Edinburgh, Scotland, 5–7 July 2004. Interscience Communications, pp 815–820
65. Lönnermark A, Ingason H The Effect of Air Velocity on Heat Release Rate and Fire Development during Fires in Tunnels. In: 9th International Symposium on Fire Safety Science, Karlsruhe, Germany, 21–26 September 2008. IAFSS, pp 701–712
66. Ingason H, Li YZ (2010) Model scale tunnel fire tests with longitudinal ventilation. Fire Safety Journal 45:371–384
67. Ingason H, Lönnermark A Effects of longitudinal ventilation on fire growth and maximum heat release rate. In: Lönnermark A, Ingason H (eds) Proceedings from the Fourth International Symposium on Tunnel Safety and Security, Frankfurt am Main, Germany, 17–19 March 2010. SP Technical research Instute of Sweden, pp 395–406
68. Ingason H, Li YZ (2011) Model scale tunnel fire tests with point extraction ventilation. Journal of Fire Protection Engineering 21 (1):5–36

69. Harmathy TZ (1978) Experimental Study on the Effect of Ventilation on the Burning of Piles of Solid Fuels. Combustion and Flame Vol. 31:p. 259–264
70. Ingason H (1995) Fire Experiments in a Model Tunnel using Pool Fires—Experimental Data. SP Swedish National Testing and Research Institute, Borås, Sweden
71. Ingason H (1995) Effects of Ventilation on Heat Release Rate of Pool Fires in a Model Tunnel. SP Swedish National Testing and Research Institute, Borås, Sweden
72. Saito N, Yamada T, Sekizawa A, Yanai E, Watanabe Y, Miyazaki S Experimental Study on Fire Behavior in a Wind Tunnel with a Reduced Scale Model. In: Vardy AE (ed) Second International Conference on Safety in Road and Rail Tunnels, Granada, Spain, 3–6 April 1995. University of Dundee and Independent Technical Conferences Ltd., pp 303–310
73. Takeda H, Akita K Critical Phenomenon in Compartment Fires with Liquid Fuels. In: Eighteenth Symposium (International) on Combustion, Waterloo, Canada, 17–22 August 1980. The Combustion Institute, pp 519–527
74. Lönnermark A Goods on HGVs during Fires in Tunnels. In: 4th International Conference on Traffic and Safety in Road Tunnels, Hamburg, Germany, 25–27 April 2007. Pöyry
75. Croce PA, Xin Y (2005) Scale modeling of quasi-steady wood crib fires in enclosures. Fire Safety Journal Vol. 40:245–266
76. Tewarson A, Pion RF (1976) Flammability of plastics. I. Burning intensity.. Combustion and Flame 26:85–103
77. Li YZ, Ingason H, Lönnermark A Fire development in different scales of a train carriages. In: 11th International Symposium on Fire Safety Science, New Zealand, 2014.
78. Drysdale D (1992) An Introduction to Fire Dynamics. John Wiley & Sons.;